1970

An experimental and theoretical evaluation of the nitrous oxide-acetylene flame as an atomization cell for flame spectroscopy

James Orley Rasmuson
Iowa State University

AN EXPERIMENTAL AND THEORETICAL EVALUATION OF THE NITROUS OXIDE-ACETYLENE FLAME AS AN ATOMIZATION CELL FOR FLAME SPECTROSCOPY

by

James Orley Rasmuson

A Dissertation Submitted to the
Graduate Faculty in Partial Fulfillment of
The Requirements for the Degree of
DOCTOR OF PHILOSOPHY

Major Subject: Analytical Chemistry

Approved:

Signature was redacted for privacy.
In Charge of Major Work

Signature was redacted for privacy.
Head of Major Department

Signature was redacted for privacy.
Dean of Graduate College

Iowa State University
Ames, Iowa

1970

TABLE OF CONTENTS

I. INTRODUCTION

Nitrous oxide-acetylene flames are extensively employed as absorption cells and as excitation sources for the spectroscopic determination of trace elements in solution. Not only are the flame temperatures comparatively high, thus facilitating atomic emission, but the "carbon-rich" N_2O-C_2H_2 flame is capable of atomizing elements that exist almost totally as monoxides in leaner or cooler flames. (The term,"carbon-rich", refers to flames in which there is insufficient oxygen to oxidize all of the carbon in the fuel to CO and/or CO_2.)

The analysis element or "analyte" in solution enters the flame as a fine mist after nebulization of the solvent. Desolvation of the droplets, volatilization of the residual particles, and dissociation of the resulting gaseous metal compounds are processes that must occur before the formation of free atoms.

The purpose of this dissertation is to examine quantitatively, both by review of the literature and by experiment, the efficiency of analyte atomization in the premixed N_2O-C_2H_2 flame. Accordingly, the topics of solute vaporization and metal compound formation as well as the extent to which processes in flames reach equilibrium will be discussed.

A. Equilibrium in Flames

A complete description of free atom production in the N_2O-C_2H_2 flame would require knowledge of the mechanism for each physical and chemical process involved in producing metal atoms from the analyte in solution. Other necessary information would include kinetic and thermodynamic data for each mechanism, an accurate and uniform flame temperature, and the concentrations of all flame species involved in the free-atom production processes. Fortunately, appropriate assumptions and approximations allow the study of the N_2O-C_2H_2 flame environment without a detailed understanding of flame propagation or free-atom formation mechanisms. The primary assumption made in this study is that thermodynamic equilibrium exists in a portion of the flame. An examination of the applicability of this supposition is, therefore, necessary.

1. General thermodynamic equilibrium

"General thermodynamic equilibrium" or "thermal equilibrium" exists in a flame when a unique temperature describes the radiation density of the flame, the distribution of energy among internal and external degrees of freedom of the flame gases, and the extent of ionization and dissociation of the flame constituents (1). Obviously, thermal equilibrium is impossible since heat, radiation, and mass are being transported from the flame (2). In addition,

flames are not strictly isothermal. At atmospheric pressure and moderately high temperatures, nevertheless, the degree of disequilibrium outside of the primary reaction zone is very slight with regard to the distribution of translational, vibrational, and electronic energies (1-7). Since a unique temperature can adequately describe the partitioning of energy among these modes even though energy is being continuously transferred to the surroundings, the flame is said to be in "local thermodynamic equilibrium". Local thermodynamic equilibrium is possible because the rate of transfer of energy between these modes is faster than the rate of energy transport from the flame. Because of the existence of temperature gradients, local thermodynamic equilibrium is a meaningful concept for only a small portion of a flame. "Local thermodynamic equilibrium" for the purposes of this discussion, will be synonomous with "general thermodynamic equilibrium" or merely "equilibrium".

Just as important as the energy distributions among internal and external degrees of freedom is the degree to which natural flame species achieve equilibrium concentrations, especially in the region of the flame normally observed in analytical spectroscopy. Unfortunately, the "degree of concentration equilibrium" in high temperature, carbon-rich flames has not been studied. To extrapolate from prior published work on cooler, leaner flames such as those formed

from O_2-N_2-H_2 mixtures is, therefore, necessary.

2. The primary reaction zone

Zones of combustion are well defined only in premixed, laminar-flow flames. In the case of premixed N_2O-C_2H_2 flames, the primary reaction zone extends at most 3 mm above the tip of the slot burner. Consideration of the nature of this zone is important to this study only to the extent that the primary reaction zone influences the degree of concentration equilibrium in the region of spectroscopic observation.

The initial reactions of a flame occur in the "primary reaction zone" (8, p. 153). A steep temperature increase of up to several thousand degrees is associated with this zone. The concentrations of minor constituents or "free radicals" may be several orders of magnitude greater than those predicted by thermal equilibrium calculations. For example, Fenimore and Jones (11) measured atomic oxygen concentrations that were factors of 2000 and 1500 above equilibrium values in the primary reaction zones of O_2-N_2-H_2 and O_2-N_2-C_2H_2 fuel-lean flames respectively. The major flame constituents, such as H_2O, CO_2, and H_2, leave the primary reaction zone at concentrations very close to those predicted by thermodynamic calculations.

3. The post reaction zone

The "post reaction zone" or "burnt-gas region" is located immediately downstream of the primary reaction zone. This is

the region that includes the interconal zone or the "red feather", which is useful for spectroscopic measurements in carbon-rich N_2O-C_2H_2 flames. In contrast to the major flame species, which enter the zone in equilibrium concentrations when the temperature is greater than ∿1300 K (2, 8, p. 152; 9-11), free radicals may be present in supra-equilibrium concentrations (8, 12-14). Nevertheless, certain relationships between the partial pressures of free radicals exist for this zone.

These relationships are a result of a pseudo-equilibrium state known as "partial equilibrium" (15). The reactions that are thought to be responsible for the establishment of partial equilibrium in the post reaction zone of H_2 and non-carbon-rich C_2H_2 flames are (8, 11, 12, 15-17):

$$H_2 + OH \rightleftarrows H + H_2O \qquad [1]$$

$$H_2 + O \rightleftarrows H + OH \qquad [2]$$

$$O_2 + H \rightleftarrows O + OH \qquad [3]$$

and

$$CO + OH \rightleftarrows CO_2 + H \qquad [4]$$

Even in the vicinity of the tip of the primary reaction zone, flame species involved in reactions [1] to [4] may achieve partial pressures that are consistent with the mass-action expressions for these reactions (8, p. 161). The attainment

of this consistency for any of these reactions implies that the free radicals of those particular reactions are in a state of partial equilibrium. Flame stoichiometries that cause both species on either side of these reactions to become very low in concentration may slow down a reaction and delay the attainment of partial equilibrium. The free radicals involved in reactions [1], [2], and [4] rapidly approach the partial equilibrium state at all stoichiometries (except possibly when a flame is carbon-rich), and $[O_2]$ reaches partial equilibrium via reaction [3] in fuel-lean flames (8, p. 161; 11, 15-18). Contributions from other possible bimolecular reactions only hastens the establishment of partial equilibrium involving [1] through [4] (12). The degree of disequilibrium of [H] and [OH] may be expressed by the relationship (brackets, [ ], refer to partial pressures)

$$\frac{[H]}{[H]_{eq}} = \frac{[OH]}{[OH]_{eq}} \qquad [5]$$

which is obtained by equating the mass-action expression for Equation [1] under complete equilibrium conditions (denoted by the subscripts eq) and for the case involving supra-equilibrium concentrations (12). A similar treatment of reaction [4] also leads to Equation [5]. The degree of disequilibrium of [O] and/or $[O_2]$ may be similarly derived from

reactions [2] and [3] when either or both of these free radicals are in partial equilibrium.

Reactions [1] through [4] are also responsible for adjusting the partial pressures of major flame species to equilibrium values. For example, addition of reactions [1] and [4] results in

$$H_2 + CO_2 \rightleftarrows CO + H_2O \quad .$$

The reason that partial pressures of free radicals sometimes persist in supra-equilibrium concentrations is because the sum of the free radicals is significantly reduced only by slow ternary collisions. If reactions [1] through [4] were the only reactions occurring in a flame, the equilibrium state could never be approached. Hydrogen and non-carbon-rich acetylene flame reactions that are responsible for the slow removal of free radicals are (2, 8, p. 156; 12-14, 16, 17, 19):

$$H + H + X \rightleftarrows H_2 + X \qquad [6]$$

$$H + OH + X \rightleftarrows H_2O + X \qquad [7]$$

$$O + O + X \rightleftarrows O_2 + X \qquad [8]$$

$$O + H + X \rightleftarrows OH + X \qquad [9]$$

and

$$CO + O + X \rightleftarrows CO_2 + X \qquad [10]$$

where X is any flame molecule acting as a third body to remove the energy of recombination.

4. Factors influencing the degree of free radical concentration equilibrium in the post reaction zone

The extent to which the concentrations of free radicals reach equilibrium in the post reaction zone is a function of the flame temperature, the nature of the fuel and oxidant, the molar ratio of oxidant to fuel, and the elapsed time since the radicals left the primary reaction zone. Measurements of the partial pressures of the H radical in O_2-N_2-H_2 flames, for example, typically indicate a marked departure from equilibrium low in the burnt-gas region, but higher in the flame, [H] approaches $[H]_{eq}$.

The effect of temperature on free radical disequilibrium is a consequence of the fact that the sum of equilibrium-predicted partial pressures of free radicals increases very rapidly with temperature. This increase is a result of increased dissociation of stable molecules into free radicals. On the other hand, the total number of free radicals produced in the primary reaction zone does not appreciably change as the temperature increases (8, p. 164). Thus, at low flame temperatures, more free radicals enter the post-reaction zone than are predicted by equilibrium calculations. Conversely, at higher flame temperatures, the equilibrium sum of

all free radicals approaches the number of free radicals produced in the primary reaction zone, and concentration equilibrium is rapidly approached, even low in the flame, via binary exchange reaction such as [1] through [4] (8, p. 161). Ample evidence of this temperature effect on free radical disequilibrium in the post reaction zone is in the literature. For example, Fenimore and Jones (10) reported that $[H]/[H]_{eq}$ was greater than 4000 at 1285 K; Schofield and Sugden found $[H]/[H]_{eq}$ equal to $\sim$3 at 2135 K and $\sim$1 at 2445 K (20). These values were measured in flames from O_2-N_2-H_2 mixtures. Thus, the post reaction zones of these flames are in thermal concentration equilibrium when the flame temperature is greater than $\sim$2500 K (8, p. 164).

At identical temperatures that are too low to produce free radical equilibrium, O_2-N_2-H_2 flames of all stoichiometries and O_2-N_2-C_2H_2 stoichiometric and fuel-lean flames have about the same degree of free-radical disequilibrium (2, 8, p. 164; 16, 17, 20, 21). Surprisingly, the addition of traces of hydrocarbons to fuel-rich O_2-N_2-H_2 flames reduces the ratio of [H] to $[H]_{eq}$ by as much as a factor of 3 (10). A striking exception to the "overshoot" phenomenon exists in non-sooting, fuel-rich hydrocarbon flames. Fenimore and Jones (10) have shown that $[H]/[H]_{eq}$ is $\sim$1 for fuel-rich (but not carbon-rich) O_2-N_2-C_2H_2 flames, even at temperatures

as low as 1600 K.

Attempting to explain this exception, Schott (15) has related the formation of supra-equilibrium concentrations of free radicals to the mole ratio of flame reactants to products. Thus for the flame reactions

$$2H_2 + O_2 \rightarrow 2H_2O$$

and

$$C_2H_2 + O_2 \rightarrow 2CO + H_2$$

these ratios are 3/2 and 2/3, respectively. Although both reactions require supra-equilibrium concentrations of free radicals to sustain combustion in the reaction zone (8, p. 155; 22, p. 92), the O_2-H_2 flame not only requires an excess of free radicals to propagate the flame, but ternary collisions are required to effect the required molar reduction of reactants to products. Since both flame reaction mechanisms are bimolecular (8, p. 155; 22, p. 92), there ought to be an approximate one to one correspondence between the number of moles of reactants and the number of moles of products entering the post reaction zone. As a result, flame systems, such as fuel-rich O_2-C_2H_2, for which the mole ratio is less than 1, are able to conform to the equilibrium state without as many slow, ternary free radical recombinations. Fuels such as CO, H_2S, CS_2, and C_2H_2 can burn to triatomic products only if sufficient oxygen is present. Thus, flame systems

incorporating these fuels can only have reactant-to-product mole ratios that are less than 1 if the flames are sufficiently fuel-rich. (This generalization does not apply to O_2-CO flames because the mole ratio is always greater than 1 for this flame.) Most other fuels burn with the mole ratio, less than or equal to 1, regardless of the flame stoichiometry. For example, the stoichiometric flame reaction for CH_4 can be written as

$$CH_4 + 2O_2 \rightarrow CO_2 + 2H_2O.$$

5. Free radical concentration-equilibrium in nitrous oxide-acetylene flames

The post reaction zone of non-carbon-rich N_2O-C_2H_2 flames ought to maintain free radical concentration equilibrium because (a) the temperature of these flames is close to 3000 K, and (b) the significant flame processes ought to be similar to those of flames from non-carbon-rich O_2-N_2-C_2H_2 mixtures.

The validity of extrapolating the results of equilibrium studies of cooler, non-carbon-rich flames to describe carbon-rich, N_2O-C_2H_2 flame processes may be somewhat questionable since these N_2O-C_2H_2 flames contain a much wider variety of free radicals. Nevertheless, such an extrapolation may provide some insight into N_2O-C_2H_2 interconal-zone flame processes. (The interconal zone is the portion of the post reaction zone that is carbon-rich.)

The primary assumption made in the experimental section of the dissertation is that virtually complete equilibrium with respect to free radical concentrations exists in the interconal zone of carbon-rich, nitrous oxide-acetylene flames. This supposition should be valid for two reasons. First, the high temperature of these flames requires that a large number of free radicals exist in the equilibrium state; thus, the equilibrium state should be attainable without a significant number of the slow, ternary collisions required to reduce the sum of free radicals. The equilibrium state is probably not approached via reactions [1] through [4] since the interconal zone contains only very minute concentrations of oxygen-containing radicals such as OH, O, and O_2. Nevertheless, other similar, rapid, binary exchange reactions may readjust the concentrations of the large number of free radicals entering the interconal zone. Secondly, fuel-rich, N_2O-C_2H_2 flames undergo an increase in the total number of moles of reactants as compared to the total number of moles of products. As indicated earlier, this increase also relieves the dependence on slow recombination reactions to achieve the equilibrium state.

6. Chemiluminescence

A supra-equilibrium population of electronic states may be caused by chemical reactions that involve flame species in supra-equilibrium concentrations. The resulting non-

thermal radiation is known as "chemiluminescence".

For example, in the post reaction zone, reactions [6] through [10] may excite the third body, X. Sugden (19) classified this type of chemiluminescence as "first category" chemiluminescence. Chemiluminescence belonging to this category occurs from electronic states up to and slightly above 5eV (23, p. 146). When free radicals and other flame species are present in equilibrium concentrations, chemiluminescence is impossible since the rate at which electronic states are populated by a chemical reaction must equal the rate at which excited states are quenched by the reverse reaction. Thus, chemiluminescence of the first category is most intense in low temperature flames in which the disequilibrium of free radicals is greatest. An increase in flame temperature or a lowering of the excitation potential of a spectral line, moreover, tends to mask all evidence of chemiluminescent excitation because the intensity of thermal emission exponentially increases with temperature as predicted by the Boltzmann equation. Consequently, low-excitation-potential lines, such as Na 5890 Å, are useful for air-acetylene, post-reaction-zone temperature measurements even when appreciable free radical disequilibrium exists (1). When chemiluminescence was significant, Gaydon and Wolfhard (24) experimentally verified a significant increase in Fe-line reversal temperatures with increases in the excitation

potential. Since line-reversal temperature measurements of N_2O-C_2H_2 flames are not a function of the excitation potential of the observed spectral line (25, 26), chemiluminescence of the first category is not significant in these flames.

The second category of chemiluminescence is restricted to the primary reaction zone of flames containing hydrocarbons (19). The intensity of this type of chemiluminescence masks chemiluminescence of the first kind. Excited states up to 8 eV may be overpopulated (23, p. 146). Although the exact mechanism for second-category chemiluminescence has been the subject of debate (19, 23, p. 146; 27-33) and is not known, the intensity of this type of chemiluminescence is proportional to the concentration of free electrons (32), which are believed to be produced by the "chemiionization" reaction

$$CH + O \rightarrow CHO^+ + e^- \qquad (34).$$

B. Vapor-Phase Metal Compound Formation and Dissociation

There is abundant speculation in the literature on N_2O-C_2H_2 flame processes and analyte atomization mechanisms in carbon-rich, high temperature flames. The best example is the often-referred-to paper on N_2O-C_2H_2 flame processes by Kirkbright, Peters, and West (35). Apparently, these authors

subscribe to the view that the concentrations of natural flame species are in a state of gross disequilibrium: they state that because a higher proportion of oxygen is introduced into air-acetylene flames, "it might be expected that this increase in the availability of oxygen might favor the formation of refractory species and that this should outweigh the ability of the hotter flame to dissociate the refractory oxides." In addition, Kirkbright et al. noted the observation of strong emission from CN and NH in the red interconal zone of a N_2O-C_2H_2 flame. From these observations, they concluded that CN and NH "predominate" in the interconal zone and are present in "great abundance" or "high concentration". Kirkbright et al. further postulated reaction mechanisms for both metal atomization and for the destruction of CN and NH, and ascribed the lifetime of CN and NH to slow reaction mechanisms rather than to the attainment of equilibrium concentrations. The reactions suggested by Kirkbright et al. for atomization of stable oxide forming elements were of the type

$$MO + NH \rightarrow M + NO + H \text{ or } M + OH + N \qquad [11]$$

and

$$MO + CN \rightarrow M + CO + N \qquad [12]$$

The data to be discussed later in this dissertation show that CN and NH should actually occur at much lower concentration

levels relative to those of other molecules that are equally capable of reducing metal monoxides.

Amos and associates (36, 37) as well as Kirkbright et al. (35) ascribed primary importance to interconal-zone reactions of the type

$$MO + C \rightarrow CO + M$$

for the enhancement of free-atom populations of elements that form stable monoxides. Although Fassel and associates (38, 39) and Gilbert (27) noted that these reactions may contribute to the enhancement effect, their interpretation relied less on speculative reaction mechanisms. Rather, they focused attention on the fact that carbon-rich C_2H_2 flames contain appreciable concentrations of carbon-containing species such as solid carbon, C_n, CH, and CN and that reactions of the type

$$C(C_n, CH, CN, \text{etc.}) + O \rightarrow CO$$

were highly exothermic. The dissociation energy of CO is significantly greater than even the most stable metal monoxides. A natural consequence of this situation is that the equilibrium

$$MO \rightleftarrows M + O$$

should be shifted far to the right in the atomic-oxygen-

depleted environment of the interconal zone, even if the metal is introduced into the interconal zone as the monoxide. Gilbert's calculations (27) showed that the atomic oxygen concentrations of sooty O_2-C_2H_2 flames are so low that virtually complete dissociation of stable metal monoxides into free atoms should occur. L'vov's (40, p. 132) and Anderson's (41) calculations predicted that atomic oxygen concentrations should decrease six orders of magnitude between stoichiometric and carbon-rich O_2-C_2H_2 flames. Anderson's predicted concentration ratios of metal to metal oxides were in essential agreement with those of Gilbert (27).

Fassel, Rasmuson, Kniseley and Cowley (42) related the degree of atomic line enhancements in carbon-rich, N_2O-C_2H_2 flames to the monoxide dissociation energies of various metals. Employing the flame model that is described in this dissertation, they calculated that atomic oxygen and atomic carbon concentrations should be abruptly inverted at the N_2O to C_2H_2 flow ratio of 2. The results of these calculations provided support for their conclusion that atomization behavior in the N_2O-C_2H_2 flame was primarily determined by the equilibrium state. Their flame was not shielded, however, and consequently, the effect of air entrainment was not known. Moreover, the organic solvent which was employed in that study, probably significantly altered their flame

stoichiometry; the precise effect of the organic solvent was unknown. Finally, comparisons between predicted metal number densities and measured absorbances as a function of the flow ratio of N_2O to C_2H_2 were performed for only low heights in the flame. Thus, any possible kinetic delay in the production of free metal atoms was not detectable. One purpose of this dissertation is to remedy some of these deficiencies.

1. Influence of free radical disequilibrium

Whether possible free radical disequilibrium among N_2O-C_2H_2 flame species would affect the degree of metal compound formation depends upon the dominant reaction mechanisms of metal compound formation and dissociation. This point can best be illustrated by two examples.

Under conditions of free radical disequilibrium in O_2-N_2-H_2 flames, Bulewicz, James, and Sugden (12) found that the concentration ratio of Li to LiOH was determined by the mass-action expression for the following reaction:

$$Li + H_2O \rightleftarrows LiOH + H \qquad [13]$$

Thus, under conditions of free radical concentration disequilibrium, the [Li] to [LiOH] ratio is higher than expected from equilibrium considerations because supra-equilibrium concentration of H drive reaction [13] to the

left. If the mechanism for LiOH formation were

$$Li + OH + X \rightleftarrows LiOH + X$$

disequilibrium of [H] would cause less Li atomization than predicted by the equilibrium state because supra-equilibrium concentrations of [H] imply supra-equilibrium concentrations of [OH] as well (Equation [5]).

An example of free radical disequilibrium that does not affect the concentration ratio of metal to metal compound is found in the formation of metal monoxides in O_2-N_2-H_2 or non-carbon-rich O_2-N_2-C_2H_2 flames. The reaction mechanisms for metal monoxide formation and dissociation are presumed to be (2, 8, p. 180; 23, p. 123):

$$M + H_2O \rightleftarrows MO + H_2 \qquad [14]$$

and/or

$$M + OH \rightleftarrows MO + H \qquad [15]$$

Since both H_2 and H_2O are major flame species especially in hydrogen-rich flames, the concentrations of both molecules should be described by the equilibrium state. Consequently, the [M] to [MO] ratio would be independent of free radical disequilibrium, if reaction [14] were dominant. If reaction [15] were dominant, then from the mass action law

$$[M]/[MO] = \frac{[H]}{[OH]K_{16}} \qquad [16]$$

where K_{16} is the metal formation constant of reqction [16]. The solution to Equation [5] in terms of [H]/[OH] when substituted for [H]/[OH] in Equation [16] yields

$$[M]/[MO] = \frac{[H]_{eq}}{[OH]_{eq} K_{16}}$$

and, thus, [M]/[MO] determined by reaction mechanism [15] is also independent of free radical disequilibrium. Experimental observations have confirmed this independence (2, 43).

Since the exact mechanism of metal compound formation and dissociation in high temperature, carbon-rich flames is unknown, the various possible disequilibria involving the flame radicals may or may not contribute to disequilibrium of the concentration ratios of metal to metal compounds. As a result, verification of the equilibration of metal compound formation would not necessarily imply that carbon-rich N_2O-C_2H_2 flames maintain free radical concentration equilibrium. On the other hand, since free radical equilibrium in the interconal zone is very probable, metal compound formation should be determined by the equilibrium state.

2. Rate of the reactions

Again, to try to gain some insight with regard to the rate of metal compound formation and dissociation in the interconal zone of N_2O-C_2H_2 flames, observations of the situation in cooler, leaner flames will be discussed.

Sugden (43) has shown that in general, bimolecular

exchange reactions, such as reaction [13], which involve metal atoms, metal compounds, and the flame gases, cause the concentration ratio of metal to the sum of metal compounds to be determined by the mass-action law even at low heights in the flame. The rapidity of these reactions is because of the low activation energy usually associated with bimolecular exchange reactions as well as the high probability of a two-bodied collision as opposed to a three-bodied collision. Surprisingly, Sugden (44) found that metal compounds, such as metal hydrides or hydroxides, with very low dissociation energies are even more rapidly equilibrated via termolecular recombinations. For example, in an air-acetylene flame, supra-equilibrium [OH] and [H] decay rapidly with height of observation in the flame. Consequently, because of the reaction

$$Cu + OH + X \rightleftarrows CuOH + X$$

[CuOH] <u>decreased</u> with height as well (45). On the other hand, because of reaction [13], the identical decay of supra-equilibrium [H] with height lead to an <u>increase</u> of [LiOH] with height. Further evidence of the rapid approach of the concentrations of free metal atoms and metal compounds to the equilibrium state is the experimental verification of the freedom of the [M] to [MO] ratio on free radical disequilibrium in O_2-N_2-C_2H_2 and O_2-N_2-H_2 flames (2, 43). That the measured

ratio was always the equilibrium value regardless of a variety of flame temperatures and stoichiometries as well as heights of observations also verifies this contention.

C. Solute Vaporization

Another important assumption made in the experimental section is that solute vaporization of the elements studied reached completion. Whether conversion of the spray droplets to the vapor phase is total depends upon a number of factors. An adequate discussion of these factors is found in reference (23). Very briefly, the flame temperature and stoichiometry, the melting and boiling points of the solid precursors of the vaporized molecules, the particle size distribution of the aerosol, the concentrations of both the analyte and the concomitant, the rise velocity of the gases, and the height of observation all influence the degree of solute vaporization. If drastic changes in any of these factors do not influence the concentration of free atoms in a flame, complete solute vaporization is probable.

Both the refinement in aerosol particle size distributions caused by removal of the largest spray droplets in the burner premixing chamber and the relatively high flame temperature contribute to the realization of complete volatilization of many elements in pre-mixed N_2O-C_2H_2 flames. The relatively few "condensed phase" or solute vaporization

interelement interferences reported for these flames provide support for this statement. Some of the most persistent condensed phase interferences in lower temperature flames are caused by phosphorous or aluminum in solution with an alkaline-earth analyte. Phosphates form an involatile compound with alkaline earths (23, p. 114-116) and the aluminum-on-Group II "chemical" interference may be caused by the occlusion of alkaline-earth cations in an involatile aluminum oxide matrix (23, p. 114-116). Using the burner described by Fiorino (46) and employed in this investigation, Becker and Fassel (47, 48) have found that the phosphate and aluminum as well as other common condensed phase interferences do not exist in N_2O-C_2H_2 flames except at extremely high concomitant concentrations. Amos and Willis (36) and Pickett and Koirtyohann (49-51) have also observed a significant reduction in the severity of solute vaporization interelement effects in this flame. The probability that solute vaporization was complete for the elements of this study will be examined in some further detail later.

D. Atomization Efficiencies (β)

One of the primary goals of this study was to measure accurately the degree of conversion of the nebulized sample into free atoms in the N_2O-C_2H_2 flame. This degree of conversion is usually identified as the β-factor and is

defined as the ratio of the concentration of free metal atoms to the concentration of that metal in all its forms in the flame volume observed by the spectrometer (52). This factor may range from 0 to 1, and may assume very different values in various flame zones.

Several techniques have been applied to measure β-factors spectroscopically in flames (52-60). Unfortunately, meaningful comparisons of β-factors are virtually impossible for several reasons. First, the reported values reflect measurements that have been performed at widely varying heights of observation and flow ratios of oxidant to fuel. For many elements, values of β are meaningful quantities only if they refer to a particular point in a specified flame at a given stoichiometry (42).

Secondly, the reliability of spectroscopically measured β-factors depends directly on the accuracy of (a) atomic transition probabilities, (b) the fraction of the amount of spray aerosol that reaches the flame through the spray chamber, and (c) the assumption that the metal in all its forms is uniformly distributed throughout the flame gases. Independently measured transition probabilities for the same atomic transition may vary as much as a factor of 4 (54); the uncertainty in measuring a spray aerosol efficiency may be

as much as a factor of 2 (54); and, the commonly made assumption (52, 53, 60) that the metal in all its forms is uniformly distributed throughout a flame that is supported on a slot burner may conservatively introduce an error of a factor of 2. This latter point can be seen from the horizontal free atom concentration profiles of Willis (54). Thus, the possibility exists that some of the β-factors that were measured by the absolute technique are in error by a factor of 16.

To eliminate β-factor uncertainties some workers (54-57) have measured spectroscopic β-factors relative to the experimental β-factor of an element that is assumed to be completely atomized. This "relative technique" reduces or removes the dependence upon quantities (b) and (c). Each relative β-factor, however, is proportional to the ratio of two transition probabilities instead of the absolute value of only one. Moreover, incomplete atomization of the reference metal will cause a systematic error in each measured β-factor, and differences in diffusion from the center of the flame between the reference element and the "analysis" element will cause uncertainties. Thus, great care must be taken in selecting the reference element.

Of concern in both the absolute and relative techniques is the use of sharp-line hollow cathode lamps as primary sources for atomic absorption determinations of β-factors

(58). The exact line profiles of the emission line from the lamp and the absorption line from the flame are difficult to calculate, and errors as much as a factor of 2 can result from these uncertainties.

Three studies of N_2O-C_2H_2 β-factors have been completed (53, 54, 60). Koirtyohann and Pickett (53) and De Galan and Samaey (60) used the absolute method; Willis (54) measured β-factors relative to those of Cu. Unlike the other workers, Koirtyohann and Pickett exclusively employed hollow cathode lamps. Comparison of all three groups of spectroscopically measured β-factors for the nitrous oxide-acetylene flame reveals their uncertainty. β-factors for elements that do not form stable compounds should be independent of flame variables. Yet, β for Na (ionization was suppressed) varied from 0.33 to 0.97; Cu, from 0.49 to 1.0; Ca, 0.34 to 2.0; Mg, 0.88 to 2.6; Au, 0.27 to 0.71; and Mn 0.38 to 0.77. Moreover, the measured β-factors cannot be easily correlated with monoxide stabilities. For example, De Galan and Samaey (60) reported 0.12 for K, which should not significantly form any compounds in this flame and a similar β-factor of 0.11 for Ti, which has a high monoxide dissociation energy of 7.2 eV (61); Willis reported a β-factor of 0.9 for V, whose monoxide dissociation energy is 6.4 eV (62).

This discussion is not meant to impugn the significance of previously measured β-factors since order-of-magnitude

estimates were often not available for certain elements. More accurate β-factors, however, for a variety of metals should prove useful in evaluating possible improvements in analytical flame spectroscopy because detection limits by either flame emission, atomic absorption, or atomic fluorescence are inversely proportional to β. Very accurate β-factors, moreover, should enable the determination of reliable metal-atom transition probabilities. Dependable β-factors should also generate renewed interest in absolute analysis (without standards) by atomic absorption as proposed by Walsh (63) and more recently by Rann (59).

E. Experimental Summary

To check the hypothesis that the degree of atomization of metals in the N_2O-C_2H_2 flame is determined by the equilibrium state, a thermodynamic model of the flame was utilized. For ten typical elements, predictions of relative metal number densities as a function of the flow ratio of N_2O to C_2H_2 were directly compared to free-atom absorbances observed in an argon-shielded N_2O-C_2H_2 flame. Comparisons were made at six different heights of observation in the flame so that any time delay in the establishment of the equilibrium state might be detected. To estimate the amount of argon entrained into the flame, relative OH absorption as a function of height in the flame was compared to predictions based on

the thermodynamic model. Finally, the degree of atomization (β) was estimated for the ten elements by modification of the flame model so that the curves of metal absorbances matched the predicted metal number density curves.

II. EXPERIMENTAL FACILITIES AND PROCEDURES

A. Apparatus

A block diagram of the components that were necessary for the measurement of either atomic or molecular absorption spectra of the flame is shown in Figure 1. Details of the individual components are listed in Table 1.

Table 1. Description of components of the absorption system

Component	Description
Monochromator	0.5 m Ebert mount Jarrel-Ash Model 82000 scanning spectrometer. Effective aperture, f/8.6. Gratings, 1180 grooves/mm blazed for 2500Å and 5000Å. Reciprocal linear dispersion, 16Å/mm in first order.
Photomultiplier detector	EMI 6256B. Spectral response type, S13. Approximate sensitivity range, 1650Å-6500Å.
Amplifier	Princeton Applied Research Corporation lock-in amplifier, model HR-8.
Mechanical chopper	Princeton Applied Research Corporation Model BZ-1 mechanical light chopper.
Recorder	Leeds and Northrup Speedomax G Model S millivolt recorder.
Primary sources	Sharp-line hollow cathode lamps operated within the manufacturers' specified current ranges. Sylvania type DXL, tungsten filament, quartz envelope, iodine vapor filled lamp for continuum absorption. Westinghouse type EDW-6V, 18A, tungsten strip filament projection lamp for reversal temperature measurements.

Table 1 (Continued)

Component	Description
Lenses	5 cm diameter, planoconvex, fused silica with focal lengths of ±2.5 cm, measured with the Hg 5460Å line.

To assure that the optical absorption measurements were restricted to the desired small cross section of the long flame, the following optical system was utilized. A 1:1 image of the primary source was focused in the center of the flame. This image was similarly refocused at the entrance slit to the monochromator. The lens closest to the monochromator was masked to a diameter of only 3 mm. The entrance slit was restricted to a height of only 1 to 2 mm. Thus, the volume of gases observed consisted of slightly distorted cones with apexes at the center of the flame and with bases no more than 2 mm in cross section at the edges of the flame.

The flow rates of N_2O and C_2H_2 were critically monitored with calibrated rotameters (Brooks Instrument Co., Model EV 1110). The gas flow metering system is shown in Figure 2 and is consistent with the suggestions of Veillon and Park (64). Further constructional details may be found in (65). Each rotameter was calibrated at the desired pressure, with a precision wet test meter (Precision

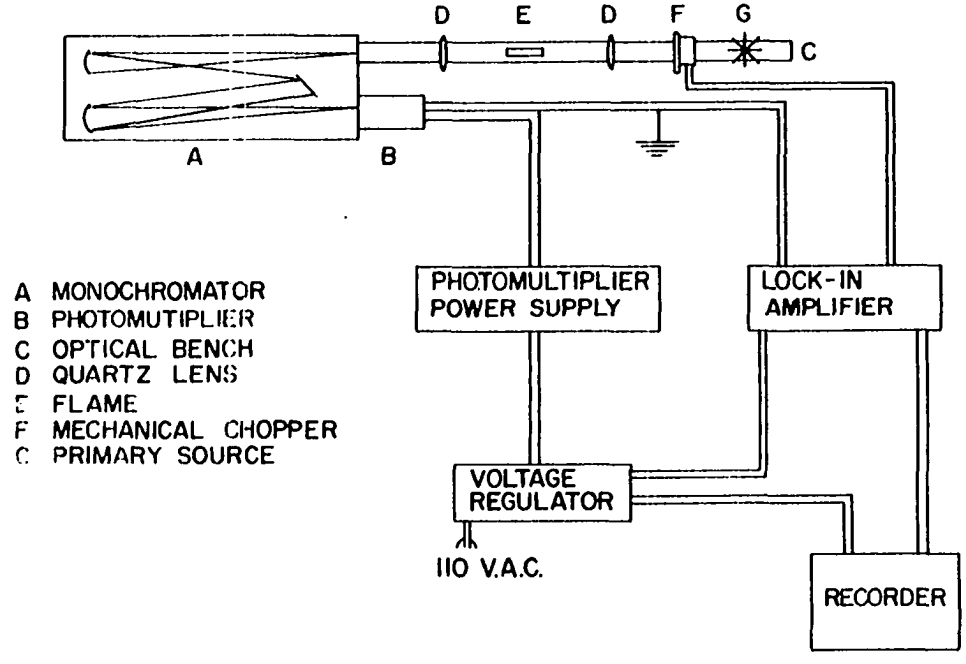

Figure 1. Block diagram of experimental facilities

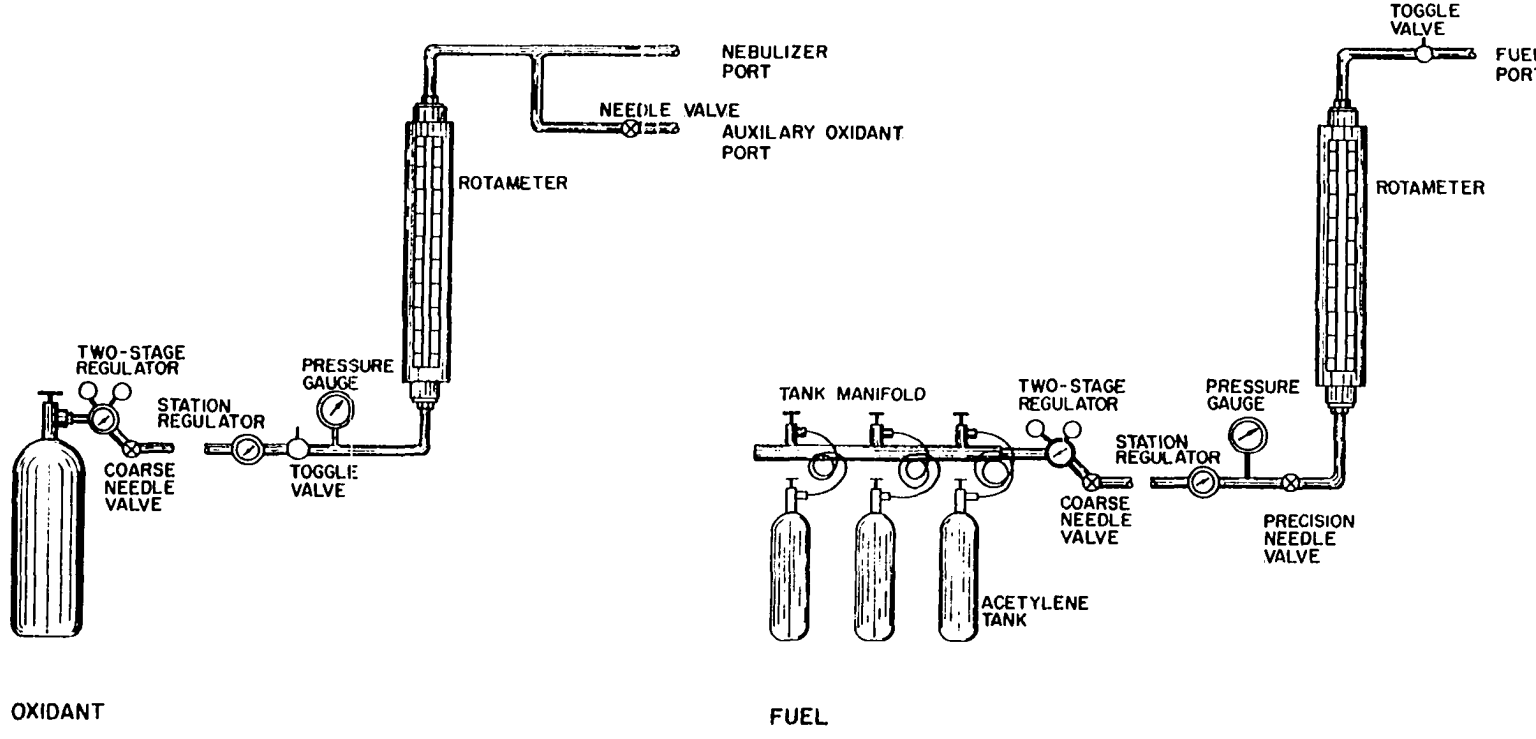

Figure 2. Flow monitoring system

Scientific). The accuracy to which the flow ratio of N_2O to C_2H_2 (ρ) could be determined was $\sim$ 1 or 2%.

The burner, which was designed (46) and modified (65) by Fiorino, provided a premixed laminar flow flame with an optical absorbing path of 7.6 cm. The burner port was not water cooled. Sealed to the base of the burner port was a water-cooled sheet metal sheath[1] that extended in height to 8.6 cm above the tip of the burner.

The purpose of this rectangular enclosure, which completely surrounded the flame, was to allow a flow of pure Ar to totally eliminate any air entrainment into the region of the flame where the spectroscopic observations were made. The sheath was water-cooled and the top of it was open to the air. The exact horizontal dimensions of the sheath were 11.5 cm in the direction of the optical path and 4.4 cm wide. Two 4 cm tall quartz windows allowed spectral observations of the flame. Two Ar ports were centrally positioned on each of the sides that were parallel to the optical path and were located 7.2 cm below the tip of the burner. First glass wool and then "BB" shot were packed into the cavity between the burner port and shield so that the argon would be evenly distributed around the flame. The "BB" shot extended almost to the tip of the burner.

---

[1]Designed by Dr. John A. Fiorino in 1969. Present address: Department of Chemistry, University of Florida, Gainesville, Florida.

B. Techniques

To cover the flow ratio (ρ) range of 1.65 to 4.65, the C_2H_2 flow was varied from 1.70 to 4.80 ℓ/min while the N_2O flow rate was kept constant at 7.90 ℓ/min. Flows of C_2H_2 in excess of 4.8 ℓ/min caused the flame to "lift-off" the burner. A portion of the N_2O flowed through an adjustable nebulizer, which aspirated 2.0 ml of solution/min. The flow of argon through the metal sheath was ∿ 19 ℓ/min.

All atomic absorption measurements were made with hollow cathode lamps as primary radiation sources and with 200 μm entrance and exit slits. Free-atom absorbances as a function of ρ were measured at selected heights by first aspirating the blank solvent and then the analyte solution while the spectrometer was "peaked" on the analysis line. The first absorbance measurement performed at each height was repeated after all others were completed to determine whether the nebulization efficiency remained constant during the course of the measurements. If agreement was not found for these two determinations all absorbance measurements at that height were repeated.

The OH absorption measurements were obtained by scanning the OH 3064 Å band-head. The quartz-iodide tungsten lamp was used as the primary source of continuum radiation. Thirty μm entrance and exit slits were employed. The fraction of light absorbed at the wavelength of maximum OH absorption was the quantity measured. This quantity was related to OH number densities in the manner described later (Section F). Each OH

absorption fraction was obtained by averaging the results of three scans.

Temperature measurements were performed by the Sr line-reversal technique described previously (25). Briefly, radiation from a tungsten strip lamp, for which the brightness temperature is known as a function of current through the lamp, is focused in the center of the flame and refocused on the monochromator slit. No mechanical light chopper is necessary because light from the lamp and emission and absorption by the flame are viewed simultaneously. The solid angle of acceptance of the monochromator must be completely immersed with radiation from the strip lamp. A limiting aperture mounted on the lens closest to the monochromator helps assure this condition. When the light from the lamp raises the flame radiation density at the wavelength of the spectral line and in the direction of the monochromator to that of a blackbody at the flame temperature, the components of the reaction

$$Sr^{*}_{(excited)} \rightleftarrows Sr_{(ground\ state)} + h\nu$$

reach equilibrium, and there is no net emission or absorption caused by the Sr atoms in the flame. If the strip lamp has a brightness temperature other than the flame temperature, emission or absorption by Sr free atoms occurs. In practice, the brightness temperature of the lamp is varied until the "null point" is reached.

Except for 50 μm entrance and exit slits, the temperature measurements were performed with the same optics used in the

absorption studies. The Sr 4607 Å line was observed while an 800 µg/ml aqueous solution of Sr was nebulized. The effect of the transmittancies of the flame sheath window and the lens, both of which were located between the flame and primary radiation source, was included in the temperature determinations. The electrical currents required to reverse the radiation emitted by the N_2O-C_2H_2 flame caused the temperature calibrations of the lamps to change considerably with use. Consequently, frequent replacement with newly calibrated lamps was necessary.

That nearly isothermal flame temperatures were measured is supported by the following arguments. First, at each selected height, the volume of gases viewed by the spectrometer from one end of the flame to the other represented a nearly "chemically uniform" environment. The contribution of the ends of the flame should have been very slight because of the long path length of radiation through the flame. Moreover, the concentration of Sr free atoms was probably lower in the region of the cool boundary layer at the ends of the flame as a result of SrO or SrOH formation (25). Secondly, since self-reversal is most significant at higher concentrations, the reversal temperatures of a flame with a large cool boundary ought to decrease with an increasing concentration of indicator metal (66). Yet, no such effect was observed with Sr. Thirdly, the measured reversal temperature is a function of the excitation potentials of the upper and lower electronic states of the indicator element in a

non-isothermal flame (26, 67). Reif (26) found that temperature measurements of a N_2O-C_2H_2 flame from a burner similar to that of this study were independent of these excitation potentials.

To eliminate the "human judgement factor" from drawing lines through experimental points, all plotted data points (except Figures 3 and 4) were connected by a second-order computer curve-fit.

C. Preparation of Solutions

The ten elements on which attention was focused in this study are listed in Table 2; the reasons for selecting this group will become apparent in the next chapter. The spectral lines selected for the absorbance measurements are also listed in the table.

The Be, Fe, and Al solutions were prepared by dissolving the powdered metals in dilute HCl; Cu metal was dissolved in dilute HNO_3; Ti powder was dissolved in dilute HF; Mg was dissolved in dilute $HClO_4$; $Na_2SiO_3 \cdot 9H_2O$, $Na_2WO_4 \cdot 2H_2O$, and LiCl were dissolved in water. All solutions were diluted with water to yield the appropriate concentrations. Potassium was added, as indicated in Table 2, to suppress ionization of the analysis element in the flame.

Table 2. Solution concentrations and wavelengths of the atomic absorption study

Metal	Line (Å)	Concentration (μg/ml)	KCl ionization suppression (μgK/ml)
Fe	3720	80	none
Li	6708	1.5	1000
Ti	3999	200	none
Na	5890	1	2000
Si	2516	400	none
Be	2349	6	none
Mg	2852	1	none
Al	3962	50	1000
Cu	3247	10	none
W	2879	325	none

D. Linearity of Analytical Curves

Since one of the goals of this study was a definitive comparison of experimental relative free-atom number densities with calculated predictions, it was important to document that measured absorbances were proportional to free-atom number densities. For the concentrations shown in Table 2, only Be and Ti exhibited non-linear absorbance-versus-concentration curves at 6 mm above the burner tip at the value of ρ that yielded maximal absorbances. Linear behavior for the Ti solutions was obtained when $\sim$ 0.3 ml of concentrated

HF was added to each (100 ml) Ti solution. Evidently, the presence of the added HF in the solutions assured maximal Ti solute vaporization (36). To correct for the possibility that the Be analytical curve was non-linear because (a) unabsorbable light from the hollow cathode fell within the bandpass of the monochromator, (b) the line from the hollow cathode was self-reversed or (c) some unknown factor other than solute vaporization inefficiencies caused the analytical curve to be non-linear, all Be absorbances were corrected so that they were a linear function of solution concentration. This correction was accomplished by extending a straight line upward from the linear region of the Be analytical curve; all measured Be absorbances were then increased by the absorbance difference between the straight line and the bent curve at the absorbance measured. If incomplete solute vaporization were responsible (23, 68, 69) for the non-linear portion of the curve, these corrections were not valid. However, the measured absorbances were at most $\sim$ 25% less than the corrected absorbances, and the corrections were not large enough to affect any of the conclusions in this manuscript.

E. Flame Characteristics

The term "fuel-rich" has often, e.g., (35, 39, 70, p. 193), been applied to flames that form a substantial, red-feather interconal zone in which the free-atom populations of stable monoxide forming elements are strikingly enhanced. It is unfortunate that this term has gained such common acceptance because, under the circumstances, "fuel-rich" is not a precise description. A stoichiometric N_2O-C_2H_2 flame may be approximated by the reaction

$$3N_2O + C_2H_2 \rightarrow 2CO + H_2O + 3N_2 \ .$$

The word "approximated" is used here because the products, especially H_2O, are slightly dissociated. This reaction implies that all values of ρ less than 3 denote "fuel-rich" flames. However, flames with ρ values between 2 and 3 do not possess the characteristics necessary for the atomization of stable monoxide forming elements. For example, at ρ equal to 2, the flame reaction may be written approximately as

$$2N_2O + C_2H_2 \rightarrow 2CO + H_2 + 2N_2 \ .$$

The flame represented approximately by this reaction may logically be described as fuel-rich. However, at this value of ρ, the extended red-feather interconal zone does not form,

and moreover, the free atom enhancements associated with high temperature fuel-rich flames are absent. Because of the abundance of molecular H_2 in the flame gases, flames possessing ρ values between 2 and 3 can more logically be identified as "hydrogen-rich". On the other hand, flames with values of ρ less than 2 contain more reactant carbon than the N_2O can oxidize to CO, and, accordingly, it is logical to identify these flames as "carbon-rich".

As indicated above, the purpose of the shielding argon flow was to prevent diffusion of air into the flame zone under observation. A number of visual observations provided strong supporting evidence of the effectiveness of this shielding. For example, a 1 cm tall interconal zone in an unshielded flame increased its height (by a factor of $\sim$ 8) to the top of the metal sheath when the argon flow was initiated. A yellow-white glow of solid carbon particles characterized the interface between the carbon-rich flame and the argon sheath. Visually, when viewed along the length of the burner slot, the center of the flame remained transparent with the typical red coloration of the interconal zone. When ρ was increased to 2, the sooty gases, which surrounded the interconal zone and extended out of the open top of the metal sheath, disappeared. Unexpectedly, a very small interconal zone of a few mm or less persisted in the hydrogen-rich flames.

The effectiveness of the Ar sheath is further supported by the following. For the sake of argument, the assumptions may be made that (a) the Ar was in some manner contaminated so that it contained 10% air and (b) that 20% of the flame gases viewed by the monochromator consisted of the contaminated Ar. Even under these exaggerated circumstances, the additional entrained oxygen would effectively increase "ρ" by less than 0.02 units.

F. Thermodynamic Flame Model

The flame model was based on the equilibrium state achieved in a closed system when C_2H_2, N_2O, and various trace metal gases are brought together and maintained at a definite temperature. To have such a model adequately describe the degree of metal atomization as both a function of ρ and height above the burner top, certain assumptions regarding both the flame and the flame model must be made. These assumptions are listed in Table 3. Most of these assumptions are defended in this chapter or the introduction. Assumptions 1 and 7 through 11 will be further defended on the basis of the experimental results. It is sufficient to state here that the most likely source of difficulty should result from incomplete fulfillment of assumptions 13 and 14. For example, a 5% error in the dissociation energy of CO would cause the calculated value for [O] in the carbon-rich flame at 2800 K to

Table 3. Major assumptions

1. Thermodynamic equilibrium exists in the flame.
2. The flame temperature is uniform over the area of spectroscopic observation.
3. The measured temperatures are accurate.
4. Entrainment of foreign gases (especially O_2) into the region of the flame where spectroscopic observations are made is negligible.
5. The partial pressures of compounds resulting from the metal salts that are sprayed into the flame are too small to influence the concentrations of natural flame species.
6. All of the metal-containing species are in the gas phase when equilibrium is complete.
7. All metal salts sprayed into the flame are completely volatilized.
8. For all values of ρ, 10% of the nebulized aerosol reaches the flame.
9. Absorbances are proportional to free metal atom number densities and are independent of temperature changes over the range of flame temperatures covered in this investigation.
10. Metal number densities in the region of the flame viewed by the spectrometer are inversely proportional to the total flow rate of the flame gases after combustion.
11. The rate of diffusion of metallic species from the center of the flame is independent of: the characteristics of each metal, flame temperature, and flame composition.
12. Ionization of all metals in the flame is completely suppressed.
13. All significant flame species are considered in the model.
14. All thermodynamic data for the significant flame species are accurate.

be in error by a factor 10.

The equilibrium concentrations of both natural and metal containing flame species were calculated in two steps. The first step consisted of calculating the partial pressures of the unsalted flame components. The second step entailed the use of the partial pressures calculated in the first step to calculate the degree of metal compound formation. Implicitly, the assumption was made that the partial pressures of metallic species were too small to influence the results of the first calculation. Because the partial pressures of metals in premixed flames are probably on the order of 10^{-7} atm, this assumption is undoubtedly valid.

1. Method of calculating the partial pressures of the natural flame species

The method of calculating the concentrations of naturally occurring flame species is similar in principle to the scheme outlined by Gaydon and Wolfhard (6, p. 288). Basically, the method consists of solving, by an iterative technique, a set of simultaneous equations that involve the conservation of mass and pressure and the mass-action expressions for the various possible flame species.

Thus, the first step in the implementation of this calculation scheme is the preparation of a list of all compounds that may be formed in this equilibration process. Although it is possible, in principle, to prepare such a complete list,

thermodynamic data are not available for all possible flame compounds. This problem is especially serious with respect to the carbon-rich flame because of the variety of carbon-containing species that may be significant. Although the list of 127 compounds shown in Table 4 is believed to include all of the major and many of the minor species which may be formed in the flame, the possibility that significant species may have been omitted is not precluded.

The latest JANAF Tables (61) were the primary source of thermodynamic data. Other investigators (8, 20, 41, 71, p. 120) have utilized these data for similar calculations. For the C_6 to C_{80} gaseous species, the data of Pitzer and Clementi (72) were utilized. These latter species could have been neglected without any effect on the model.

Table 4. Gaseous species considered in the flame - composition calculation

GRAPHITE (solid)	C_2H_4	CHO	H	NO	NH_2
C_1-C_{80}	CN	CH_2O	H_2	NO_2	NH_3
CH	HCN	C_2H_4O	O	NO_3	N_2H_2
CH_2	NCN	HNCO	O_2	N_2O	N_2H_4
CH_3	CNN	CO	OH	N_2O_3	HNO
CH_4	CNC	CO_2	H_2O	N_2O_4	HNO_2 (cis)
C_2H	C_2N_2	CCO	N	N_2O_5	HNO_2 (trans)
C_2H_2	C_4N_2	C_3O_2	N_2	NH	HNO_3

The occurrence of graphite in Table 4 needs an explanation. According to Gaydon and Wolfhard (6, p. 188, 189) the crystal structure of soot in flames is that of graphite. The crystal is slightly distorted because of the inclusion of $\sim$ 1% by weight of hydrogen. To what extent the presence of hydrogen may alter the thermodynamic data for pure graphite is not precisely known. To further complicate matters, solid carbon formation in air-hydrocarbon flames is a form of disequilibrium (6, p. 181; 73, p. 68). Carbon luminosity may occur at O to C ratios (defined as the ratio of the number of gram atoms of O in the flame gases to the number of gram atoms of C) that are too large to liberate solid carbon under equilibrium conditions. The only air-hydrocarbon flame that forms solid carbon near the expected O to C ratio of 1 is air-acetylene, in which soot forms at the O to C ratio of 1.2 (73, p. 69).

In spite of these complications, soot was not believed to be present in the center of the N_2O-C_2H_2 flame at the values of ρ employed in this study for the following reasons. First, soot was visibly absent from the center of the flame over the entire stoichiometry range. Secondly, as a hydrocarbon flame temperature increases, the "critical ratio", defined as the ratio of O to C at which carbon formation just occurs, tends to approach the "equilibrium" value (74). Over the range of stoichiometries covered in this investigation,

the calculations based on the flame model predicted that graphite formation either should not occur or should not be significant up to 26 mm above the burner tip. Above this height, the calculations predicted significant graphite formation for carbon-rich flames. As a result, experimental comparisons were not performed above this height when the results depended upon whether soot was formed. The third reason is related to the atomization behavior of metals in the flame gases and will be discussed in the next chapter.

The partial pressures of a nitrogen-containing species, a hydrogen-containing species, an oxygen-containing species, and a carbon-containing species and appropriate formation constants are adequate to calculate the partial pressures of any of the remaining gaseous species of Table 4. Thus, out of the 126 gaseous species, N_2, H_2, O, and C were selected as reactants in the mass-action expressions. The choice of these molecules as reactants in these equations was arbitrary since the equilibrium state of a system is independent of the reaction path. The set of mass-action equations, therefore, numbered 122. To allow the solution of the 122 mass-action expressions for a system with 126 variables, four additional equations were required. These equations involved the conservation of mass and pressure as follows:

$$p = 1 \text{ atm} = [N_2] + [CO] + [H_2O] + [HCN] + \ldots \qquad [17]$$

$$\frac{n_N}{n_O} = 2 = \frac{2[N_2] + 2[N_2O] + [HCN] + [N] + \ldots}{2[O_2] + [N_2O] + [OH] + \ldots} \qquad [18]$$

$$\frac{n_N}{n_C} = \rho = \frac{2[N_2] + \ldots}{[CO] + [CO_2] + [HCN] + 2[C_2H_2] + \ldots} \qquad [19]$$

$$\frac{n_N}{n_H} = \rho = \frac{2[N_2] + \ldots}{2[H_2O] + [OH] + [H] + 2[H_2] + \ldots} \qquad [20]$$

where p is the total pressure of the system and n refers to the number of moles of the subscripted element. At partial pressures of C from which graphite should form, the degree of such formation must be included in the denominator of Equation [19].

To simplify the formidable task of solving a set of 126 simultaneous equations, the iterative technique outlined by Gaydon and Wolfhard (6, p. 228) was modified and programmed in FORTRAN. Our technique is outlined in Table 5. The actual input data for the calculations were the flame stoichiometry (ρ) and the measured flame temperature. Measured flame temperatures rather than adiabatically calculated temperatures were used for two reasons. First, heat losses to the burner head can cause significant deviations between theoretical and actual temperatures (75). Secondly, the

Table 5. Nitrous oxide-acetylene iterative flame-composition calculation

1. Equilibrium constants with N_2, H_2, C, and O as reactants were calculated for the species of Table 4.

2. Starting values for $[N_2]$, $[H_2]$, [O] and TM, the total number of moles produced in the flame reaction were arbitrarily selected. (The number of moles of available N_2O as well as TM was normalized by the assumption that 1 mole of C_2H_2 was introduced into the system.)

3. [C] was varied until the calculated total number of gram-atoms of carbon in the system was made to equal the number of gram-atoms (2) of carbon introduced into the system; the orginal arbitrary values of $[N_2]$, $[H_2]$, and [O] were used in the calculation. (The four unknown variables for this particular case are not $[N_2]$, $[H_2]$, [O] and [C], but $[N_2]$, $[H_2]$, [O], and TM. TM is necessary to convert partial pressures of the carbon species to the total number of gram-atoms of carbon in the system.)

4. The partial pressures of all atoms and molecules not containing carbon were calculated. (These calculations used the arbitrarily assigned values of $[N_2]$,$[H_2]$ and [O].)

5. To cause the arbitrary value of [O] to more closely approach the true equilibrium value, [O] was changed to [O] times the ratio of the number of gram-atoms (ρ) of oxygen introduced into the system to the sum of the number of gram-atoms of oxygen determined from the calculated partial pressures. (Thus, when the mass balance for oxygen was satisfied, [O] was not changed.) Similarly, $[N_2]$, and $[H_2]$ were varied. TM assumed the new value of TM times the sum of all the calculated partial pressures. (Thus, as Equation [17] was satisfied, TM stopped varying.)

6. Steps 3, 4, and 5 were repeated until all calculated partial pressures became constant. For the calculations of steps 3 and 4, the most recently assigned values of $[N_2]$, $[H_2]$, [O], and Tm were used.

7. The resulting partial pressures were inspected "by hand" to assure that all species were related to one another in equilibrium proportions.

temperature was required as a function of height in the flame. It is recognized that the nebulized solvent contributed hydrogen and oxygen to the flame gases. According to Willis (76), $\sim$ 10% of the aerosol reached the flame for the particular spray chamber used in this study. The assumption was made that this figure applied equally well for the different gas flows and rates of nebulization that were employed in this study. It should be pointed out, however, that a $\pm$ 50% error in the estimated fraction of solvent reaching the flame would introduce less than $\pm$ 0.8% error in $\frac{n_N}{n_O}$ of Equation [18] and less than $\pm$ 1.6% error in $\frac{n_N}{n_H}$ of Equation [20]. Equation [19] would be unaffected.

2. Method of calculating the degrees of atomization for metals in the flame gases

The second step of the flame model calculations was to use the calculated partial pressures of natural flame species to predict the degrees of metal atomization as both a function of ρ and height above the burner (flame temperature). The metal-containing species (of the ten elements of this study) for which thermodynamic data was available from the JANAF Tables (61) are summarized in Table 6. This list does not represent all the possible compounds that the ten elements might form in the N_2O-C_2H_2 flame, but includes most of the more significant metal-containing species and many compounds of minor importance. No solid or liquid species are included

Table 6. Metal-containing species considered in the calculations

Si	Ti	W_4O_{12}	AlH	BeOH	MgH	LiOH
Si_2	TiO	WH_2O_4	AlC	$Be(OH)_2$	MgN	LiON
Si_3	TiO_2	Al	Be	BeH	Cu	LiH
SiO	W	AlO	BeO	BeH_2	Cu_2	LiN
SiO_2	WO	Al_2O_2	Be_2O_2	Fe	CuO	Na
SiH	WO_2	Al_2O	Be_3O_3	FeO	Li	Na_2
SiN	WO_3	AlOH	Be_4O_4	$Fe(OH)_2$	Li_2	NaO
Si_2N	W_2O_6	HAlO	Be_5O_5	Mg	LiO	NaOH
SiC	W_3O_8	AlO_2H	Be_6O_6	MgO	Li_2O	NaH
Si_2C	W_3O_9	AlN	Be_2O	MgOH	Li_2O_2	NaCN
SiC_2						

in Table 6 because "saturation effects rarely seem to play a role in limiting the extent of volatilization in flame methods" (23, p. 109), and based on JANAF Table data (61), solids and liquids involving metal species of this study were found to be unstable at total metal partial pressures of 10^{-7} atm.

The first part of the computer program (to calculate the degrees of metal atomization) consisted of calculating equilibrium formation constants for the species of Table 6. The particular metal atom, N_2, H_2, O, and C were the arbitrary reactants in the mass action expressions. Thus, the calculated partial pressures of N_2, H_2, O, and C and the measured flame temperature were required input data. The partial pressure of each metal was then varied until the calculated total metal content per unit of flame volume was equivalent to the metal content per unit of volume of the pure metal gas at 10^{-7} atm. Since metal-containing species that contained more than one metal atom did not contribute significantly to the total partial pressure of the metal and its compounds, the last sentence is equivalent to stating that the free atom partial pressure for each element was varied until the total partial pressure of the metal in all its forms was 10^{-7} atm. Consequently, the instability of compounds containing more than one metal atom caused a lack of dependence upon the assumed partial pressure of the

metal in all its forms. For example, the equilibrium ratio of [Na] to [NaO] is only a function of the atomic oxygen concentration and the temperature, but the ratio of [Na] to [Na_2] is a function of the partial pressure of Na. The "reasonable" value of 10^{-7} atm for the assumed partial pressure of the metal in all its forms would have to be at least 4 orders of magnitude larger before the predicted formation of metal compounds containing more than one metal atom would become significant.

Because metal partial pressures as a function of ρ were required, the exact value of 10^{-7} atm for the assumed partial pressure of the metal in all its forms was used only for the most fuel-rich flame at each height above the burner. At other values of ρ, an equivalent amount of metal was assumed to enter the flame. Since the ratio of the number of moles of flame reactants to the number of moles of products as well as the total N_2O-C_2H_2 flow rate changed as a function of ρ, these two quantities were also input data that were required to calculate metal partial pressures as a function of ρ. These partial pressures then had to be converted to relative number densities before meaningful comparisons could be made with the measured relative metal absorbances; this conversion was accomplished by accounting for changes in the flame volume because of variations in temperature with ρ. Thus, if the calculated

metal number densities should be expected to agree with the experimental results, the assumption (10 of Table 3) that metal number densities in the center of the nitrous oxide-acetylene flame are inversely proportional to the flow rate of the flame gases after combustion must be valid.

Oddly enough, the measured flame temperatures did not greatly influence the calculated degree of metal atomization for any element except Si. A buffering effect - a decrease in the flame temperature causes a metal monoxide formation constant to increase but at the same time the calculated [O] decreases - greatly reduced the temperature dependence of the calculations (Assumptions 2 and 3 of Table 3). The O_2-C_2H_2 flame calculations of Anderson (41) also showed this buffering effect: the calculated degree of atomization for Ti was largely independent of temperature even at air-acetylene flame temperatures. It should be pointed out, however, that in practice, Ti atomization in an air-acetylene flame at any stoichiometry is very poor (39).

3. Method of relating calculated OH partial pressures and OH fractional absorptions to OH ground state number densities

So that the amount of argon entrainment into the center of the flame might be estimated, calculated OH ground state number densities were compared with relative experimentally determined values. The relationship

$$[OH]_D \propto [OH]/Q_{OH}T \qquad [21]$$

where $[OH]_D$ refers to the OH number density in the ground state (electronic, rotational, and vibrational), Q_{OH} is the internal portion function for OH, and T refers to the flame temperature, was used to convert calculated OH partial pressures to relative number densities in the ground state. The appearance of T in relationship [21] corrects for changes in flame volume with temperature and division by the OH internal partition function compensates for the number of OH molecules not in the ground state. Thermodynamic data required for the calculation of Q_{OH} were taken from the JANAF Tables (61).

An empirical calibration curve of calculated relative $[OH]_D$ as a function of the maximum fraction of light absorbed from the OH ground state 3064 Å transition was constructed from data obtained at 6 mm from the tip of the burner. The OH absorption fractions and the corresponding calculated $[OH]_D$, values were varied by changing ρ at this height. The resulting calibration curve was used to convert measured OH fractional absorption values to experimental $[OH]_D$ values as a function of height above the burner for various stoichiometries. Finally, these experimental $[OH]_D$ values were compared on a relative basis to those predicted by the calculations of the flame model as a function of

height.

This somewhat unsatisfactory method of obtaining an OH relative number density calibration curve was necessary because the resolution of the spectrometer did not permit the complete separation of the ground state rotational component from other nearby rotational lines. Thus, integrating only over the spectral line that originated from the electronic, vibrational, and rotational ground states was impossible. To further complicate matters, even if such an integration were possible, the effects of self-absorption would not be known.

III. RESULTS AND DISCUSSION

A. Flame Temperatures

The temperatures employed in the calculations discussed above were all based on the measurements displayed in Figure 3. The unexpected temperature increase at a ρ value of 2 for the 3 mm curve may have been caused by Sr chemiluminescent emission because the primary reaction zone grew larger as the flame become carbon-rich and extended into the field of view of the monochromator.

The effectiveness of the argon shield in eliminating entrained air from the carbon-rich flame is apparent from Figure 3. The shielded flame had a steady temperature decrease with increasing height whereas an unshielded, carbon-rich flame (25) maintains a nearly constant flame temperature over heights of several centimeters. Thus, the constant temperature of the unshielded carbon-rich flame was apparently caused by secondary combustion with entrained air.

B. Degree of Argon Entrainment

If substantial amounts of Ar were entrained into the center of the flame, the effect would be similar to reducing the pressure of the flame gases, and the equilibrium partial pressures of natural flame species would consequently be altered. Because calculations based on the flame model predicted that OH partial pressures ought to be inversely

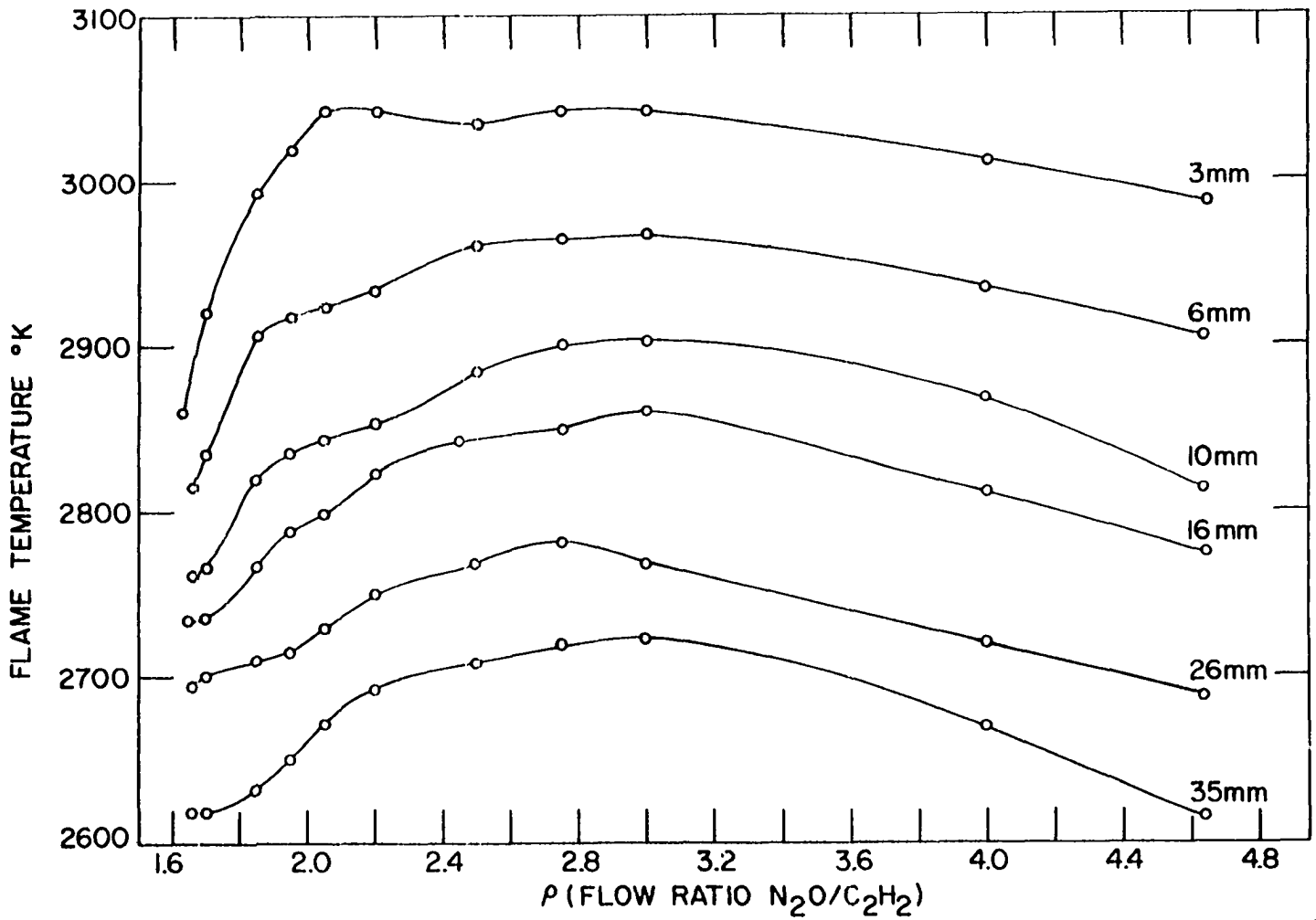

Figure 3. Argon-shielded nitrous oxide-acetylene flame temperatures as a function of ρ and height above the burner tip

proportional to the partial pressure of entrained Ar, an increase in the degree of Ar entrainment with height would cause equilibrium [OH] to decrease correspondingly more rapidly. Figure 4 shows the results of matching the relative experimental and equilibrium OH ground state number density curves discussed earlier. Both theoretical curves at ρ values of 2.5 and 3.0 were drawn under the assumption that no Ar was entrained into the center of the flame. Consequently, the entrainment of Ar into the center of the flame was assumed to be negligible because of the reasonable agreement found in Figure 4. The results of Figure 4,nevertheless, do not preclude the unlikely possibility that significant amounts of Ar entered the central region of the flame only at the base of the flame. The slight disagreement between the two curves at ρ equal to 3.0 may have been caused by a small degree of Ar entrainment or slight OH disequilibrium.

Expectedly, Figure 4 suggests that major departures from concentration equilibrium do not occur in the post reaction zone of the hydrogen-rich flames. This conclusion is based on Equation [5] and similar equations that can be derived from reactions [2] and [3]. Figure 4, however, would be more convincing if the experimental and equilibrium curves were not plotted relatively but on an absolute basis. Similar curves unexpectedly deviated from each other at values of ρ greater than 3. Fortunately, stoichiometries which are that fuel-lean are not especially analytically use-

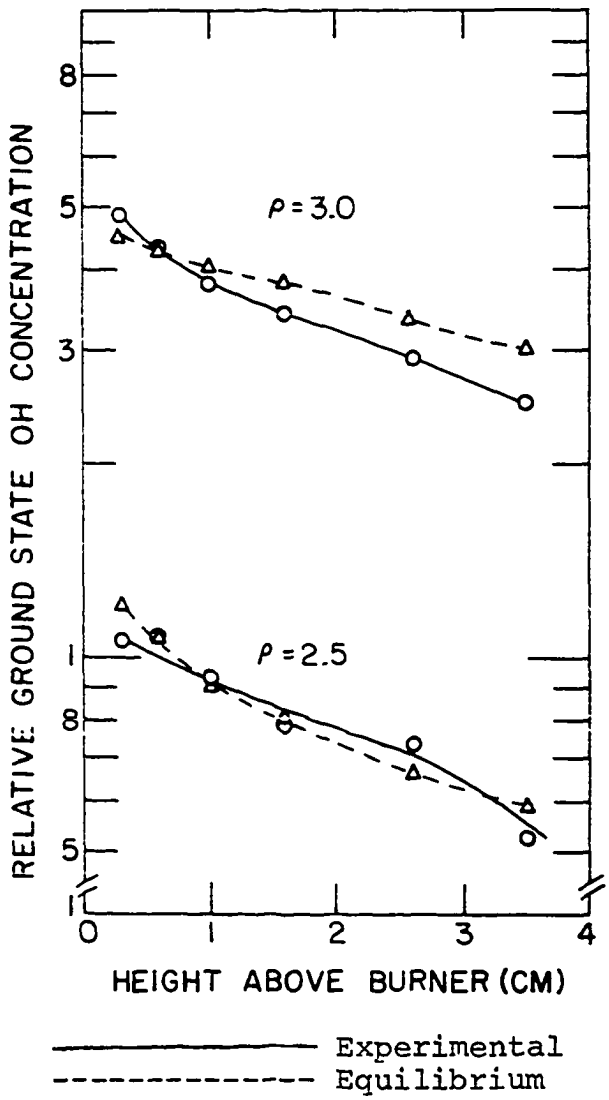

Figure 4. Relative ground state OH concentrations as a function of height in the flame

ful, and, consequently, all subsequent experiments and calculations were limited to ρ values less than 3.

C. Major Natural Flame Species

The flame model calculations yielded the composition results plotted in Figure 5. These results were calculated with the temperatures at 6 mm above the burner tip since analytical measurements are often performed at this height. The plot includes only those species that contribute at least 0.1% of the flame gases at some point in the ρ range examined. Figure 5 shows that $[N_2]$ and [CO], the major components, as well as [H] and $[H_2]$ are not particularly sensitive to ρ whereas the partial pressures of all other components are strikingly sensitive to this parameter. The data for ρ greater than 2.5 may be compared with the results reported by Jenkins and Sugden (8, p. 174). If allowance is made for the differences in the flame temperatures, the results are in basic agreement.

1. Nature of the interconal zone

The deductions by Kirkbright *et al.* (35) that "... CN...along with NH persists through the whole zone and is present in great abundance", are not totally supported by our calculations. Although CN and similar carbon-containing free radicals should *persist* in the interconal zone, CO, N_2,

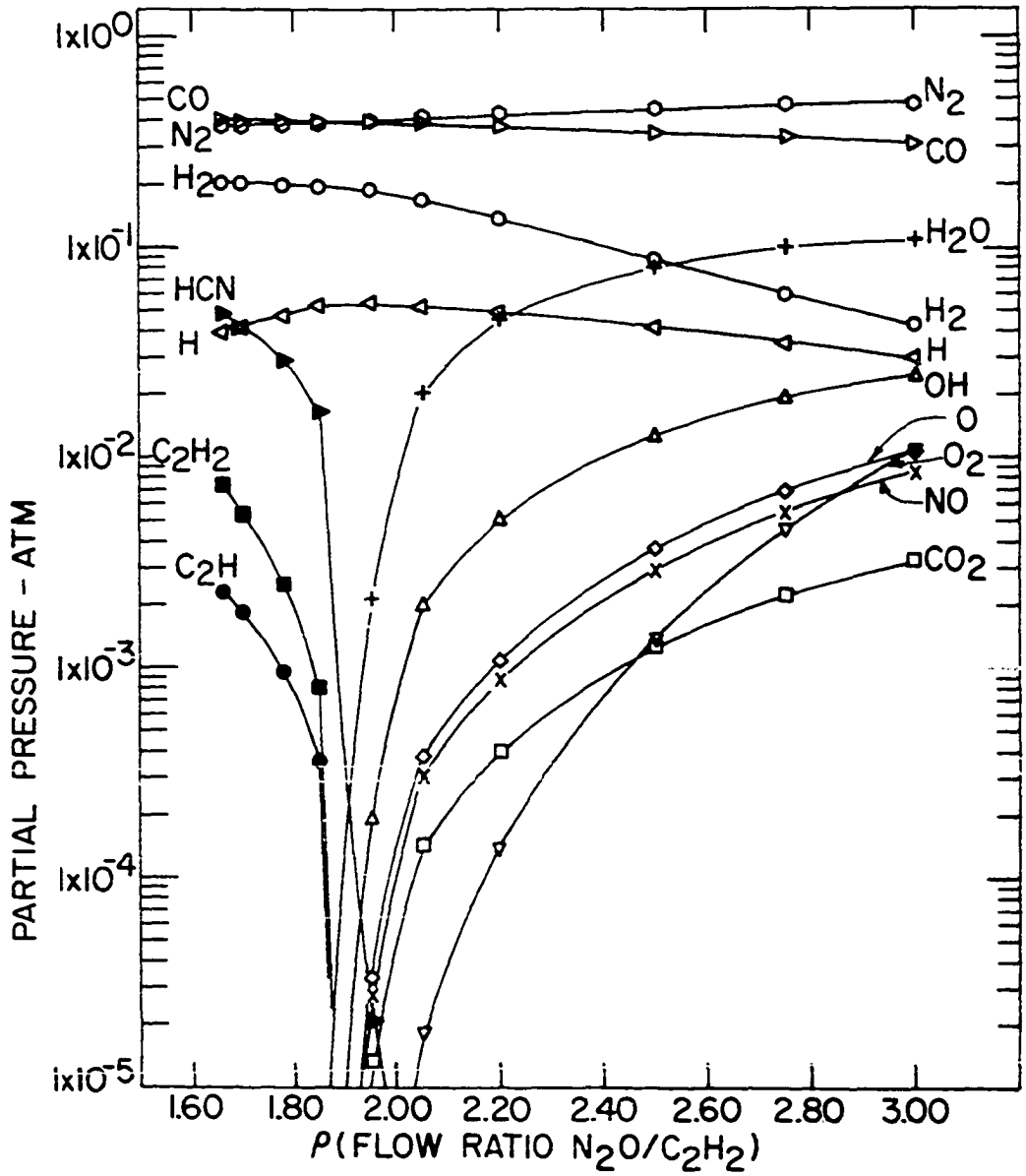

Figure 5. Equilibrium partial pressures of major nitrous oxide-acetylene species at 6 mm above the tip of the burner as a function of ρ

H_2, HCN, H, C_2H_2, and C_2H should occur in larger concentrations than CN or NH. The partial pressures of CN and NH are shown in Figure 6 along with other spectroscopically observed (35, 65) species. The relatively small partial pressures calculated for CN, C_2, CH, and NH, even though these species strongly emit from the flame, points to the dangers in overemphasizing their importance. An interesting curiosity is that the molecule, CNC, should have about the same partial pressure as CN in the carbon-rich flame.

The real significance of the CN molecule may be in its ability to form CN^-. With the concentration of CN predicted at 6 mm at ρ equal to 1.66, and with thermodynamic data from the JANAF Tables (61, released 1970) for CN, CN^-, and an electron, the ratio of the partial pressures of free electrons to CN^- was predicted to be 0.56. The equilibrium

$$M \rightleftharpoons M^+ + e^-$$

may thus be forced to the right to compensate for electron losses because of CN^- formation. Bulewicz and Padley (77) have discussed the behavior of CN as an electron acceptor in low pressure flames.

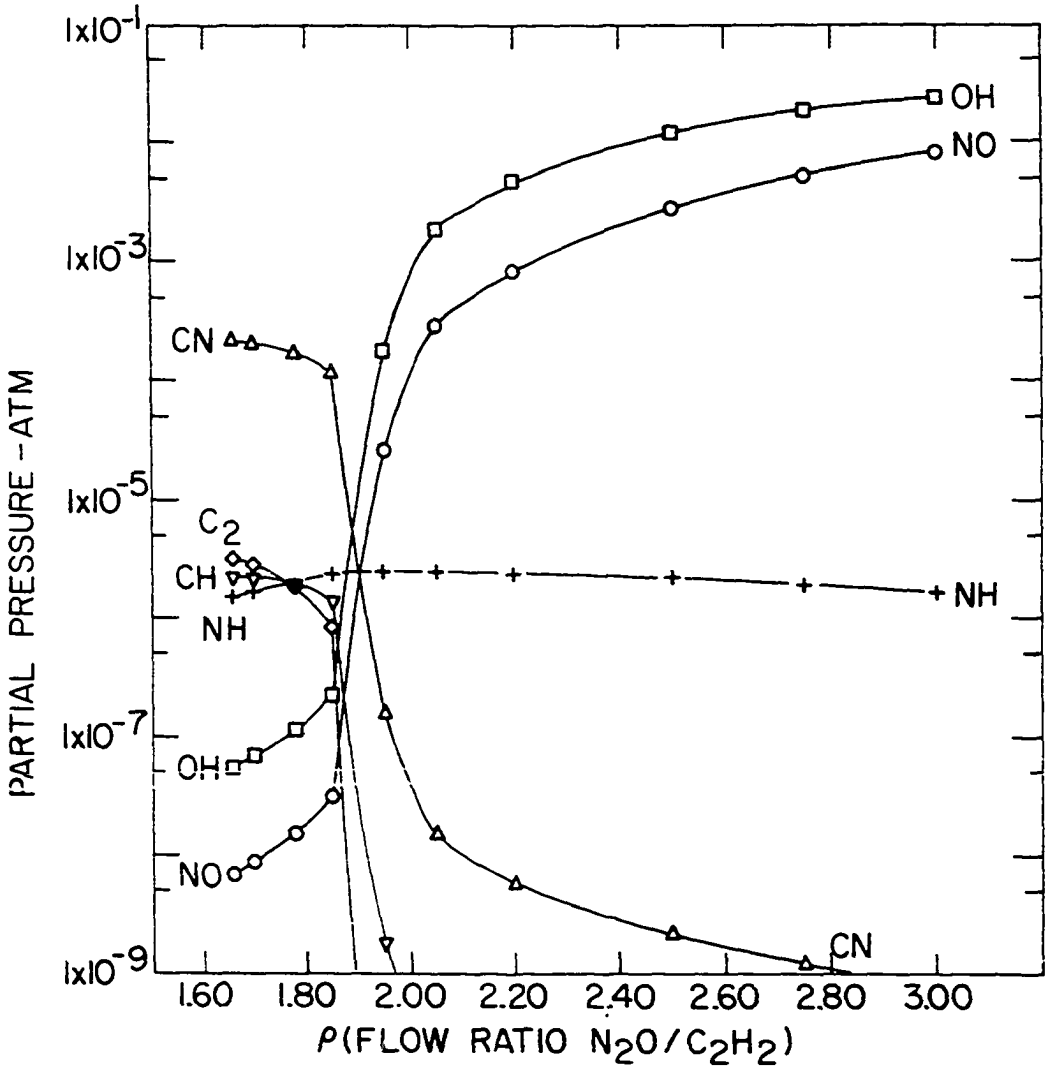

Figure 6. Equilibrium partial pressures of some spectroscopically observed flame species as a function of ρ. These partial pressures are based on temperatures measured at 6 mm

D. Metal Compound Formation

One of the major goals of this study was to compare, as a function of ρ, the theoretical predictions of relative free-metal-atom populations with the experimental observations. These comparisons, as well as predicted metal-compound number densities as a function of ρ are presented graphically in Figures 7 through 23. All absorbance and predicted metal number density curves are plotted relatively on a logarithmic scale so that direct comparisons of the shapes of the curves can be made. The arrangement of the figures is in the order of increasing proclivity of the ten metals to form compounds in the flame.

When included, the figures showing the degree of metal-compound formation as a function of ρ are placed directly following the metal absorbance and number density curves for that particular element. The only compounds included in these figures were those calculated to be present as 1% or more of the sum of all forms of that metal at least at one point in the range of ρ values considered. These figures (Figures 11, 13, 15, 17, 19, 21, and 23) were drawn from calculations in which the measured temperatures at 6 mm above the burner were employed. The computer program was so written that 1 on the number density scale of these figures corresponds to complete metal compound formation for the gas flows corresponding to the most fuel-rich flame (ρ=1.66).

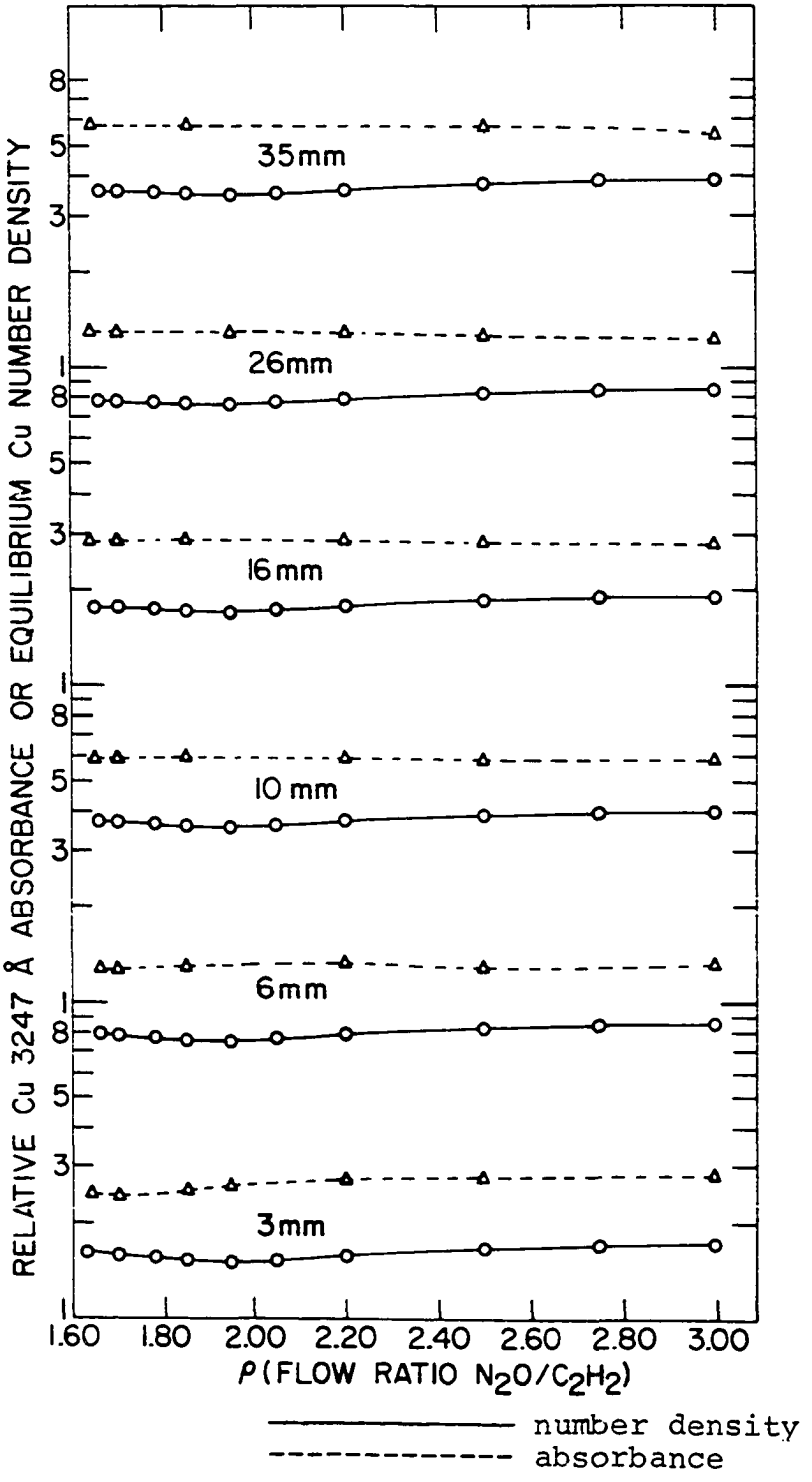

Figure 7. Relative Cu absorbances and predicted metal number densities at selected heights above the burner as a function of ρ

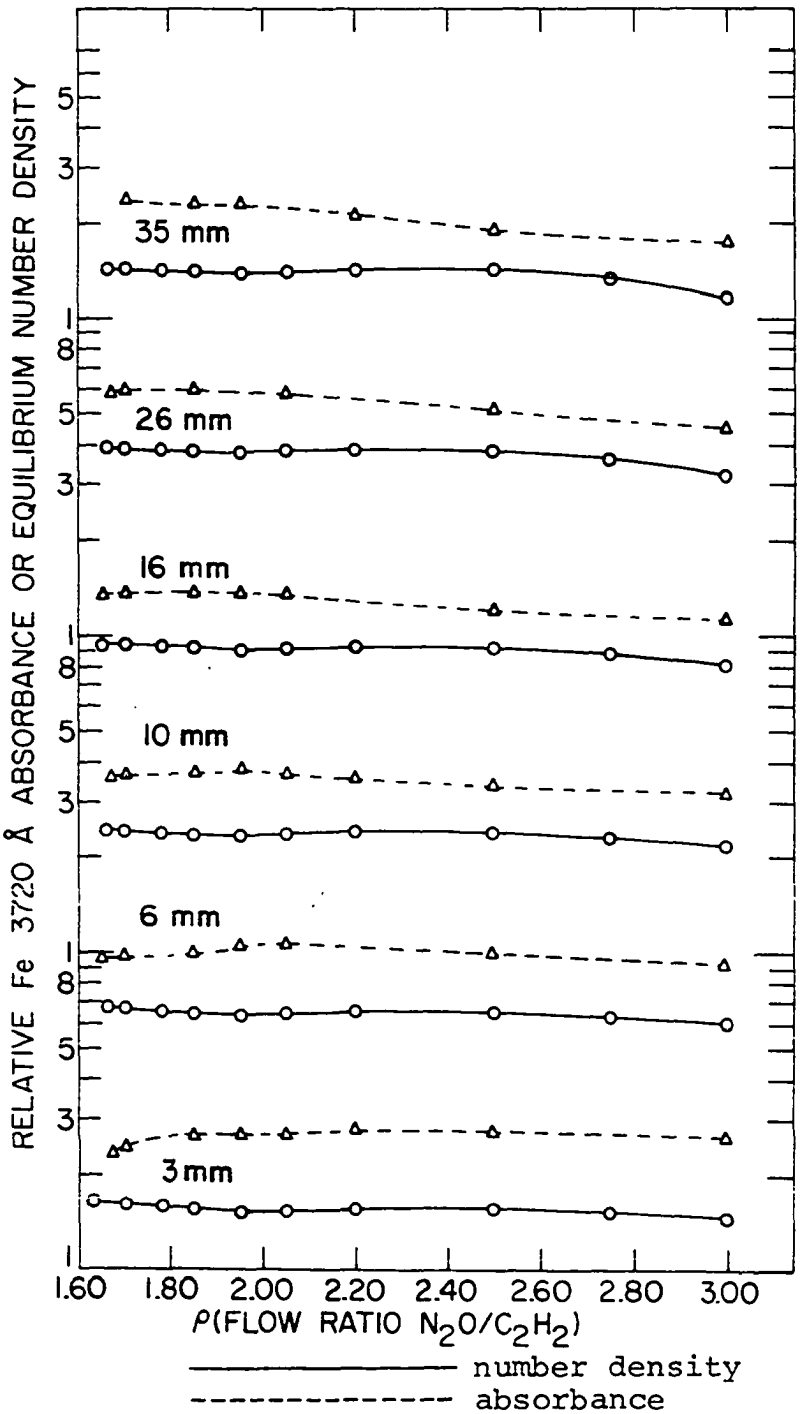

Figure 8. Relative Fe absorbances and predicted metal number densities at selected heights above the burner as a function of ρ

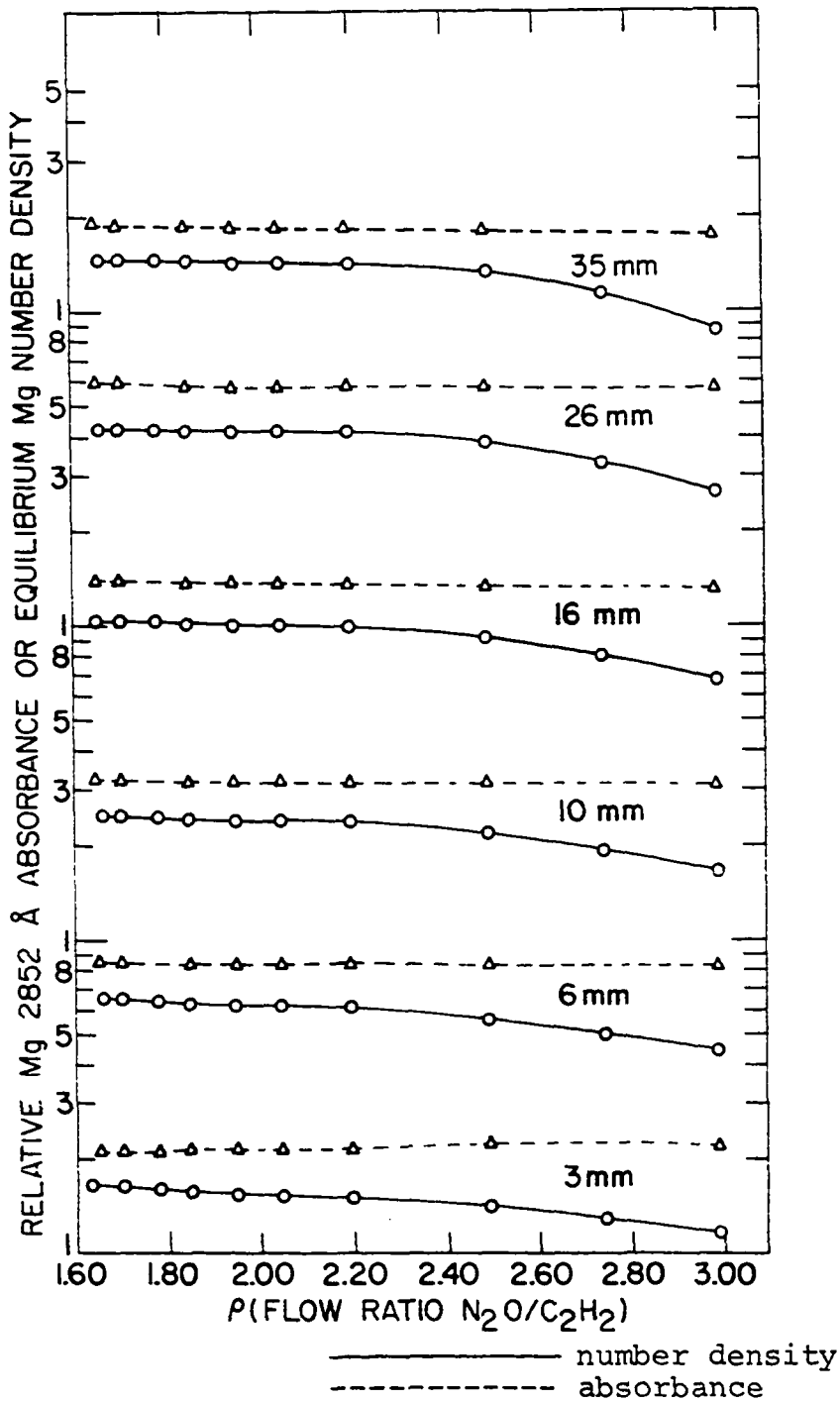

Figure 9. Relative Mg absorbances and predicted metal number densities at selected heights above the burner as a function of ρ

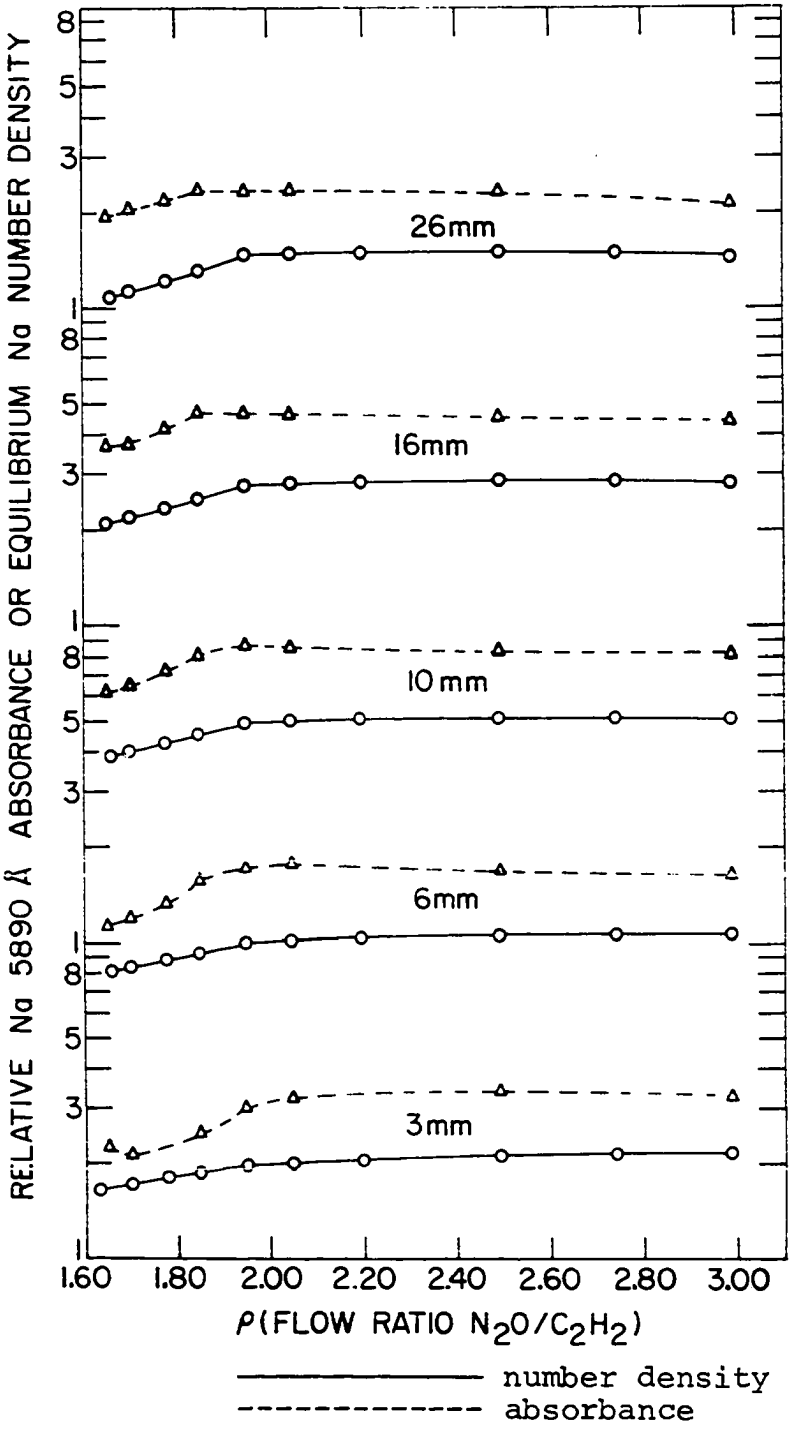

Figure 10. Relative Na absorbances and predicted metal number densities at selected heights above the burner as a function of ρ

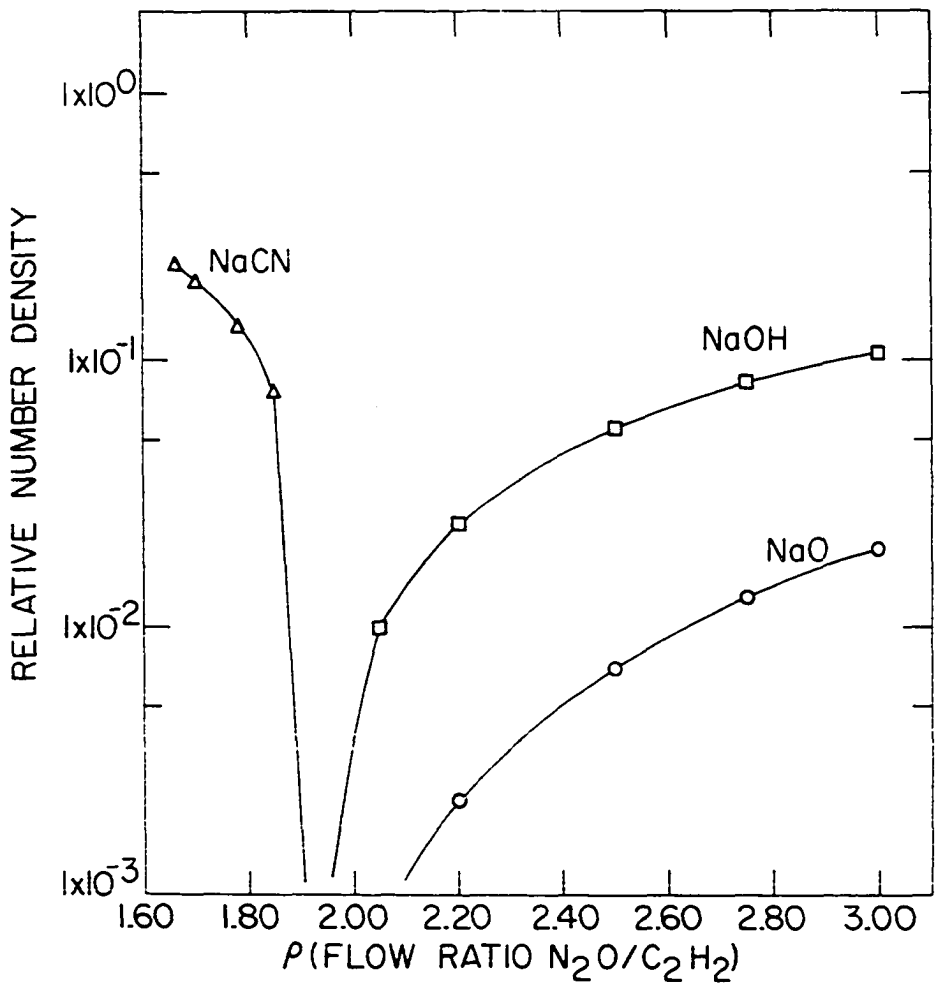

Figure 11. Predicted Na compound formation at 6 mm above the burner as a function of ρ

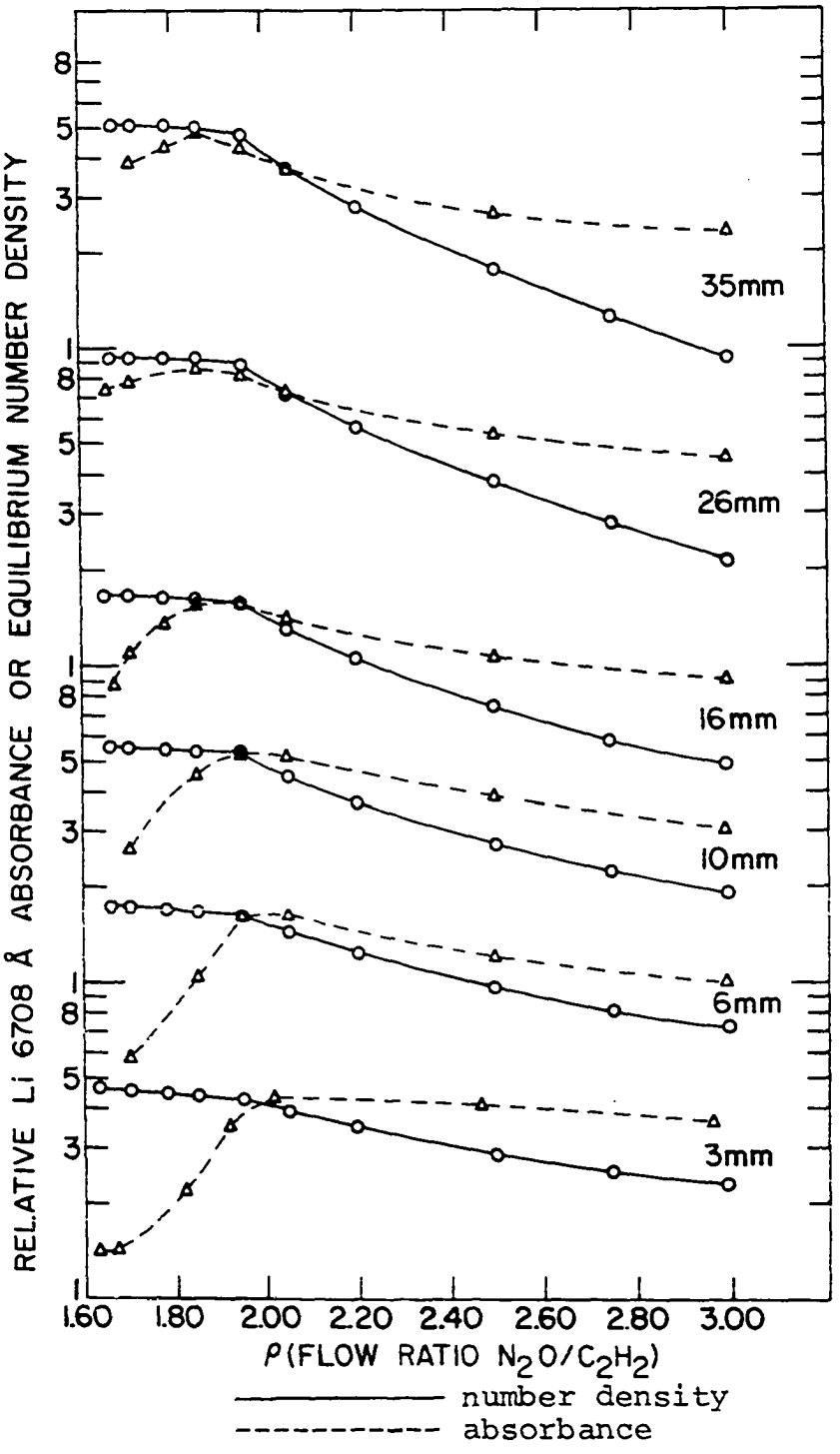

Figure 12. Relative Li absorbances and predicted metal number densities at selected heights above the burner as a function of ρ

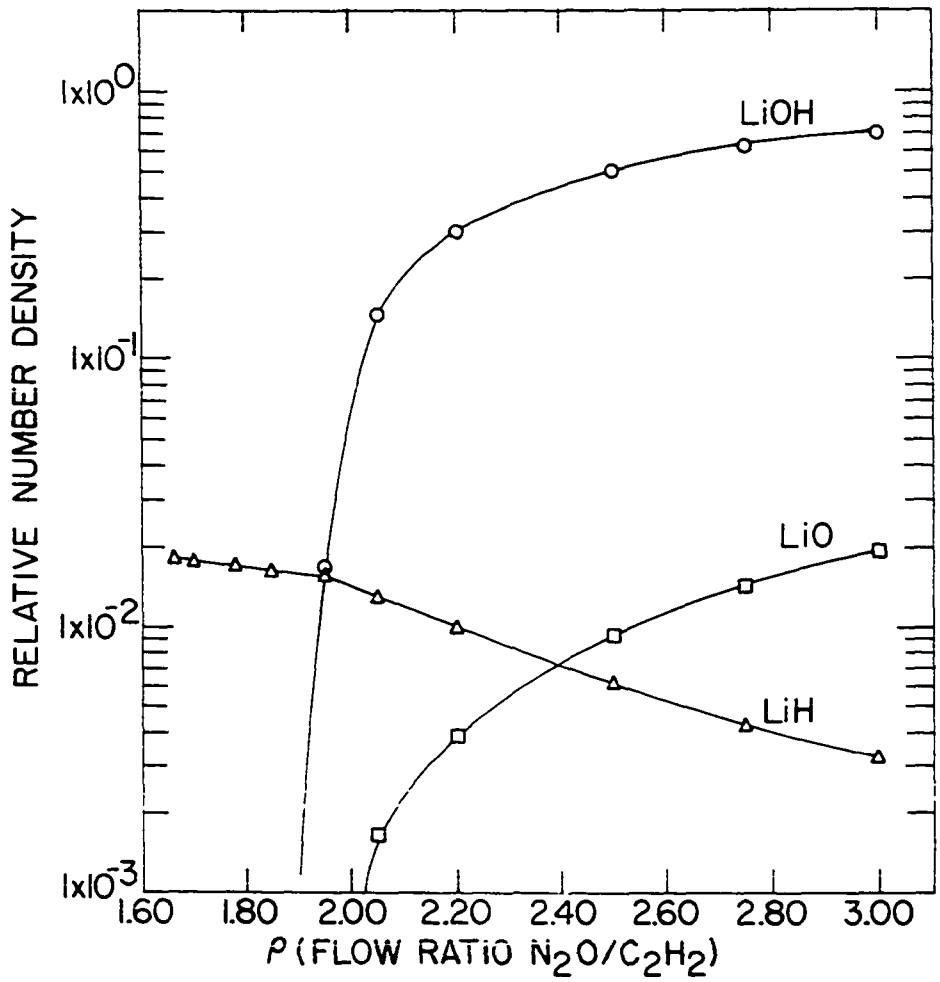

Figure 13. Predicted Li compound formation at 6 mm above the burner as a function of ρ

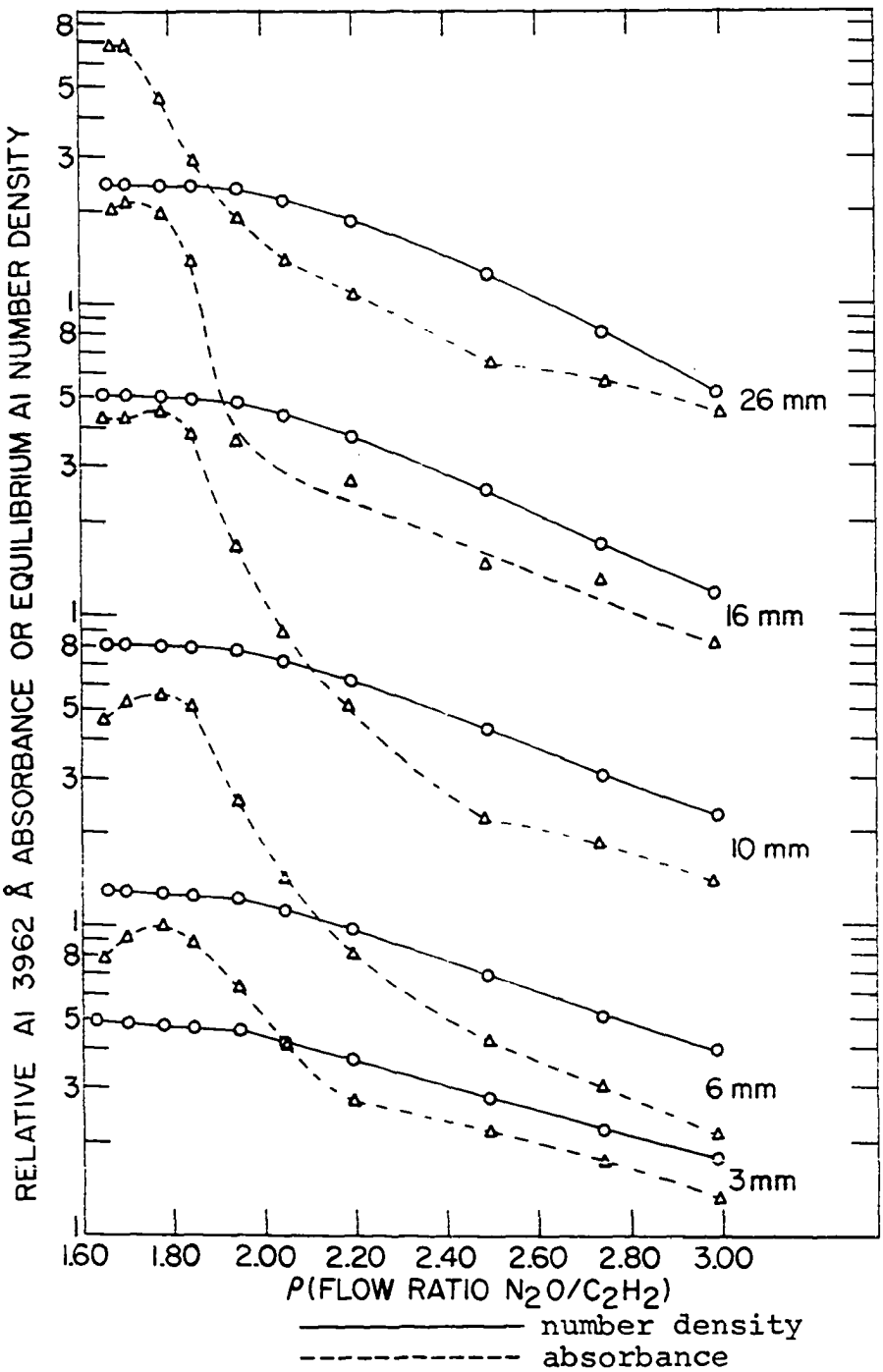

Figure 14. Relative Al absorbances and predicted metal number densities at selected heights above the burner as a function of ρ

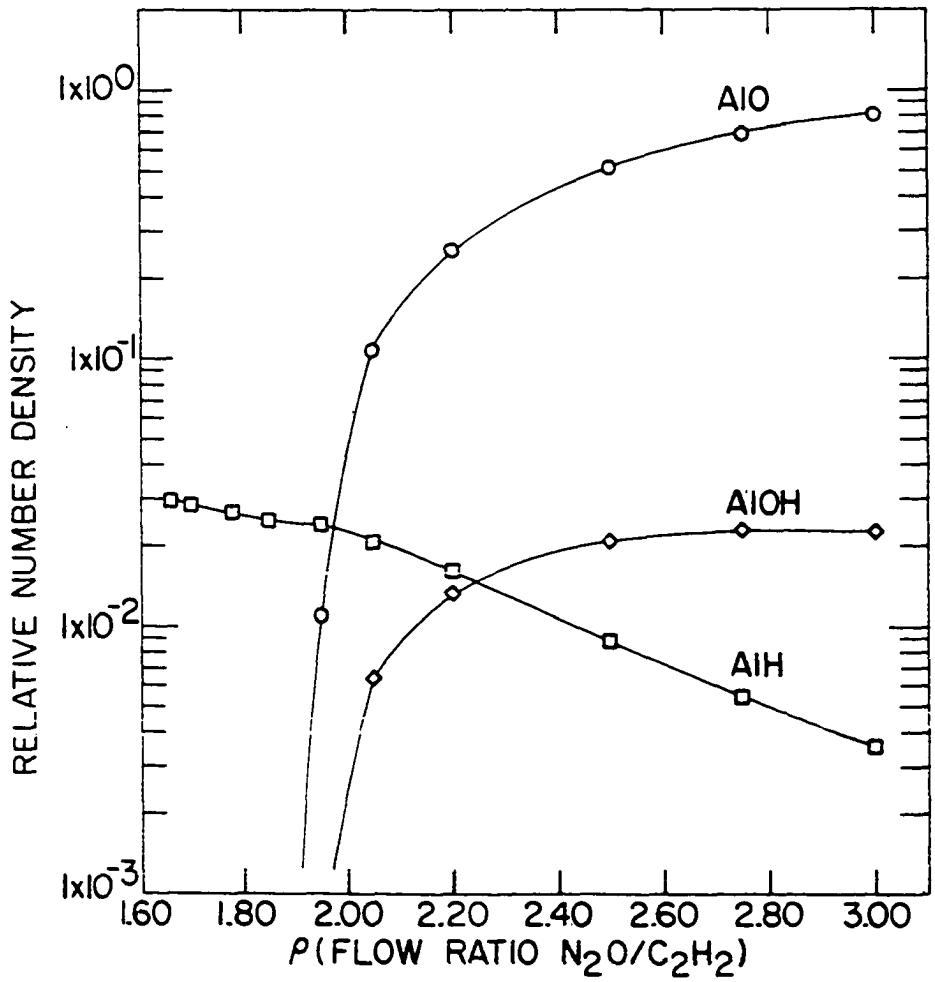

Figure 15. Predicted Al compound formation at 6 mm above the burner as a function of ρ

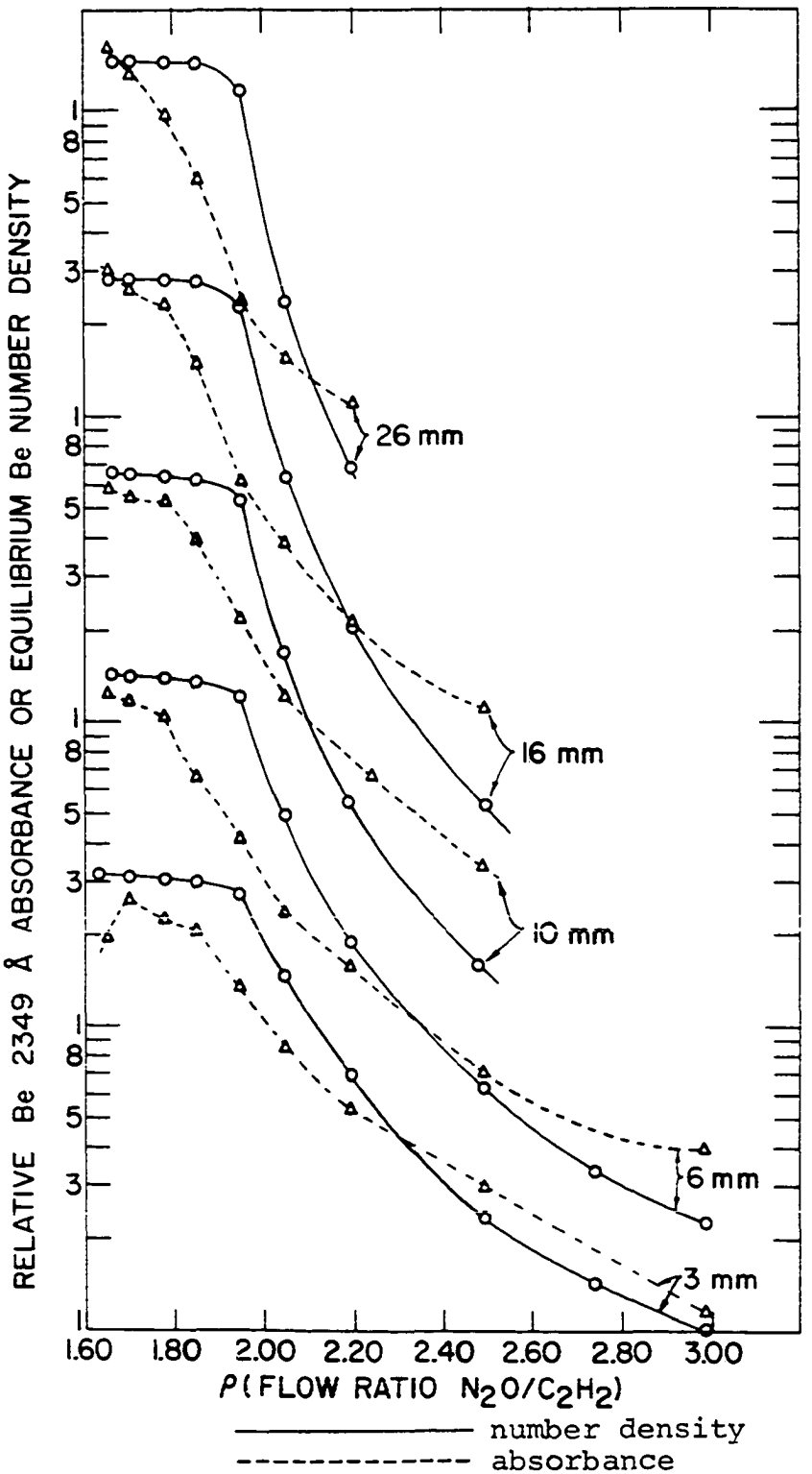

Figure 16. Relative Be absorbances and predicted metal number densities at selected heights above the burner as a function of ρ

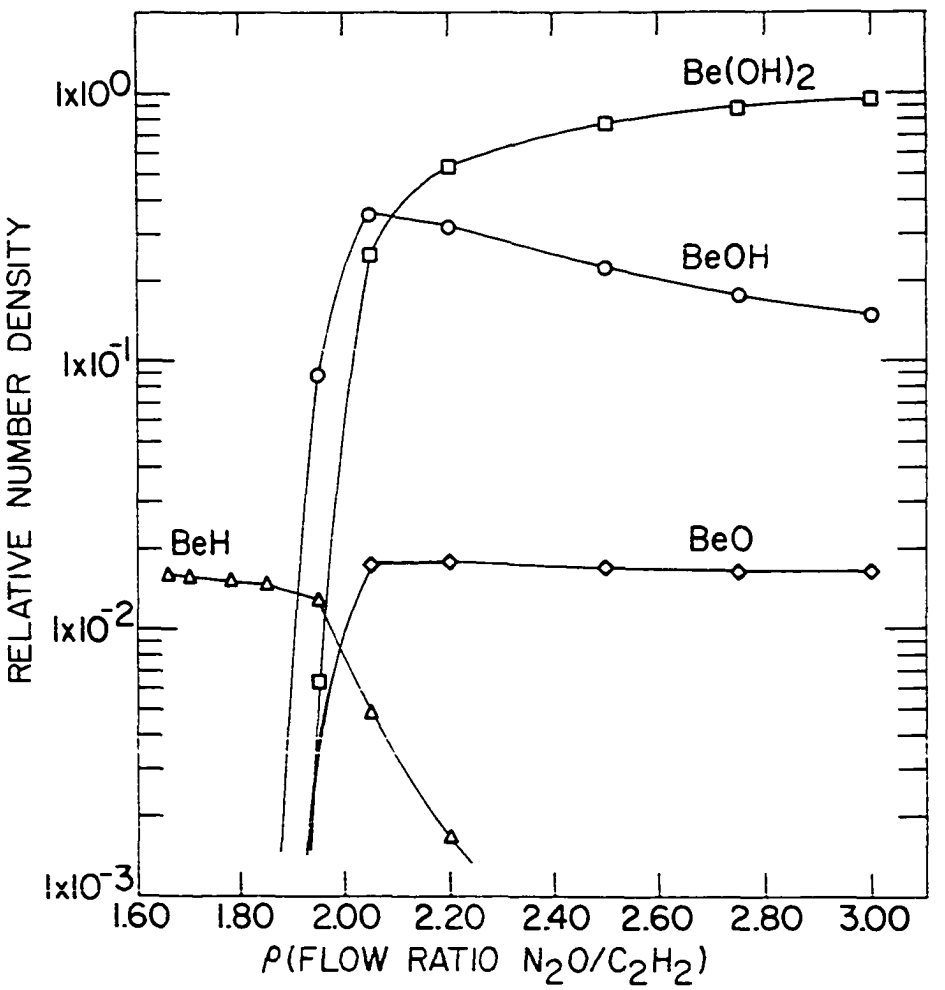

Figure 17. Predicted Be compound formation at 6 mm above the burner as a function of ρ

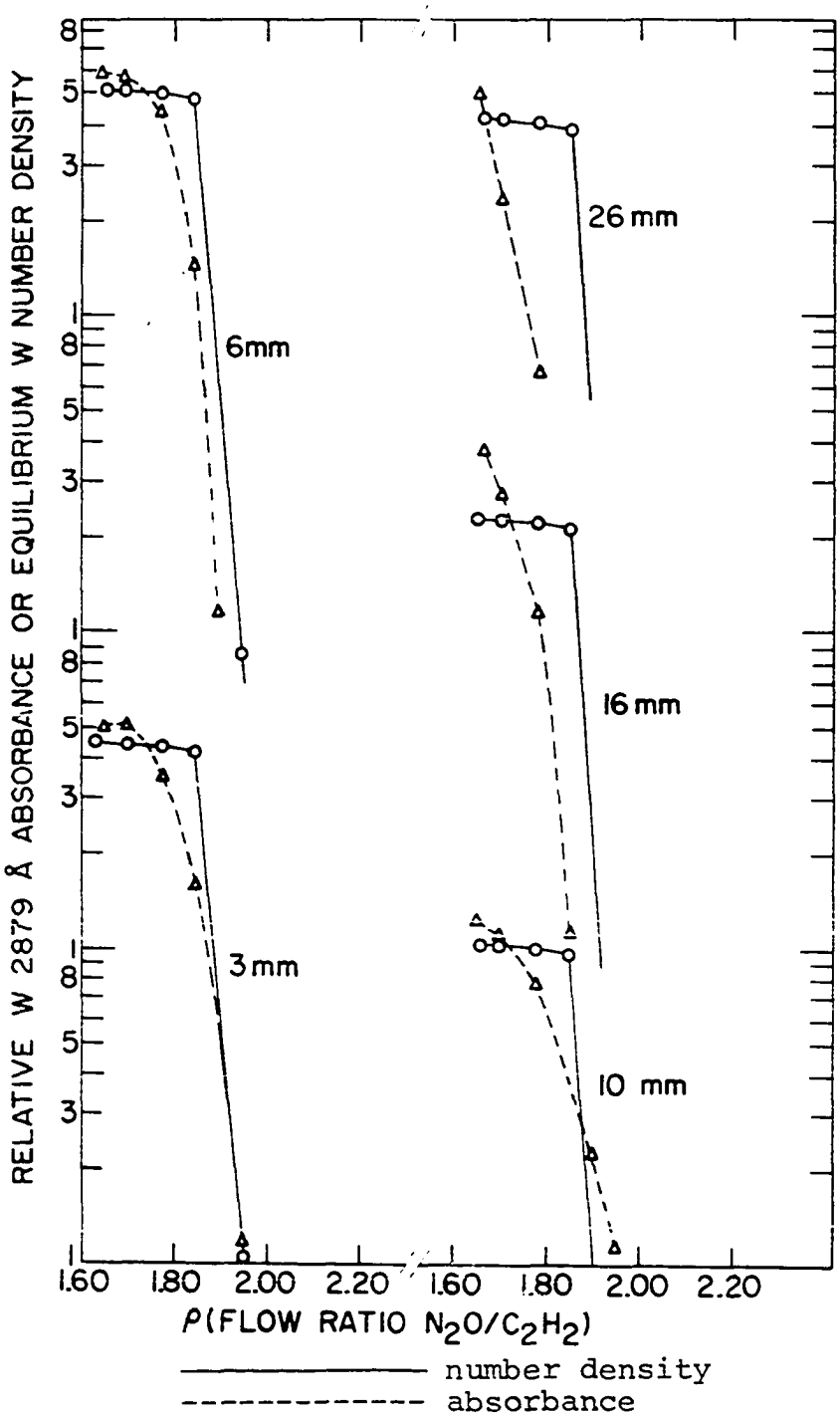

Figure 18. Relative W absorbances and predicted metal number densities at selected heights above the burner as a function of ρ

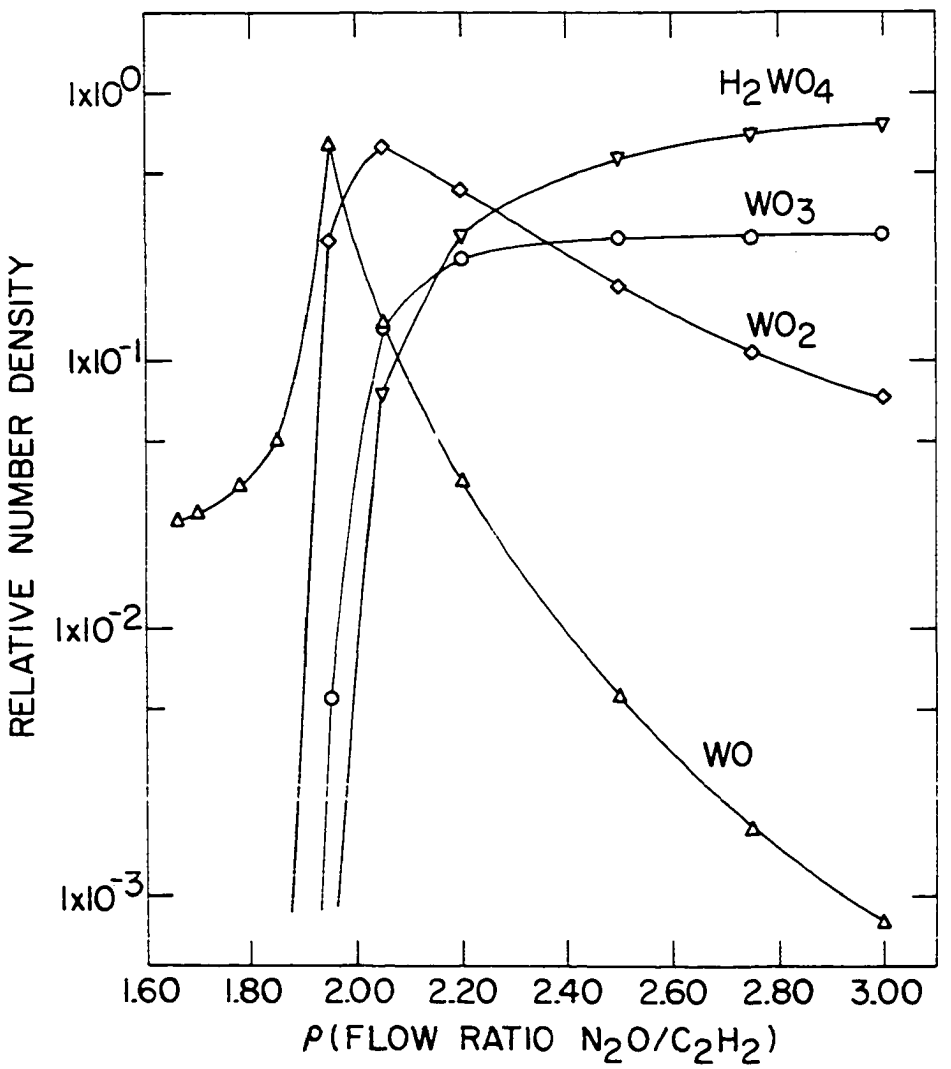

Figure 19. Predicted W compound formation at 6 mm above the burner as a function of ρ

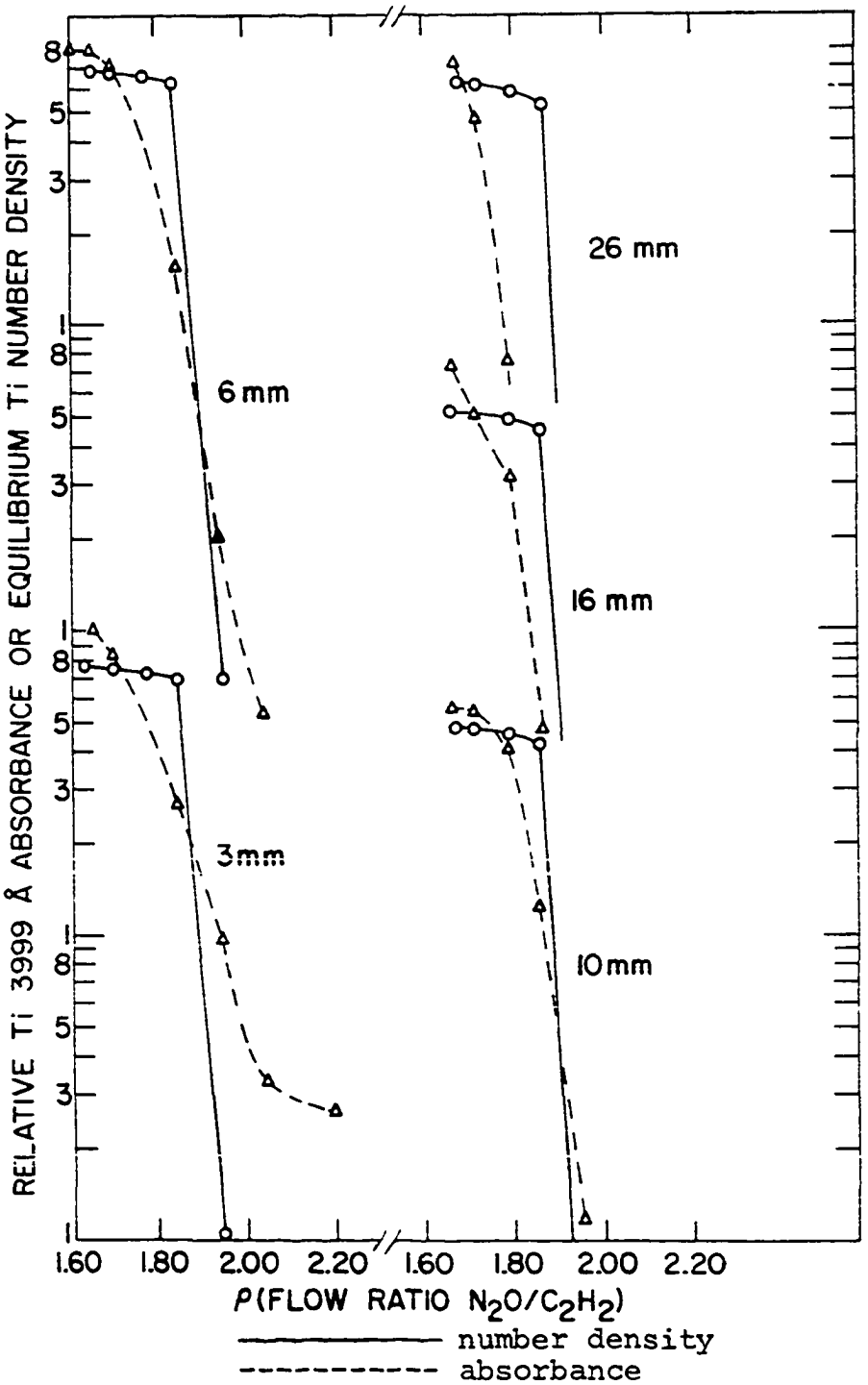

Figure 20. Relative Ti absorbances and predicted metal number densities at selected heights as a function of ρ

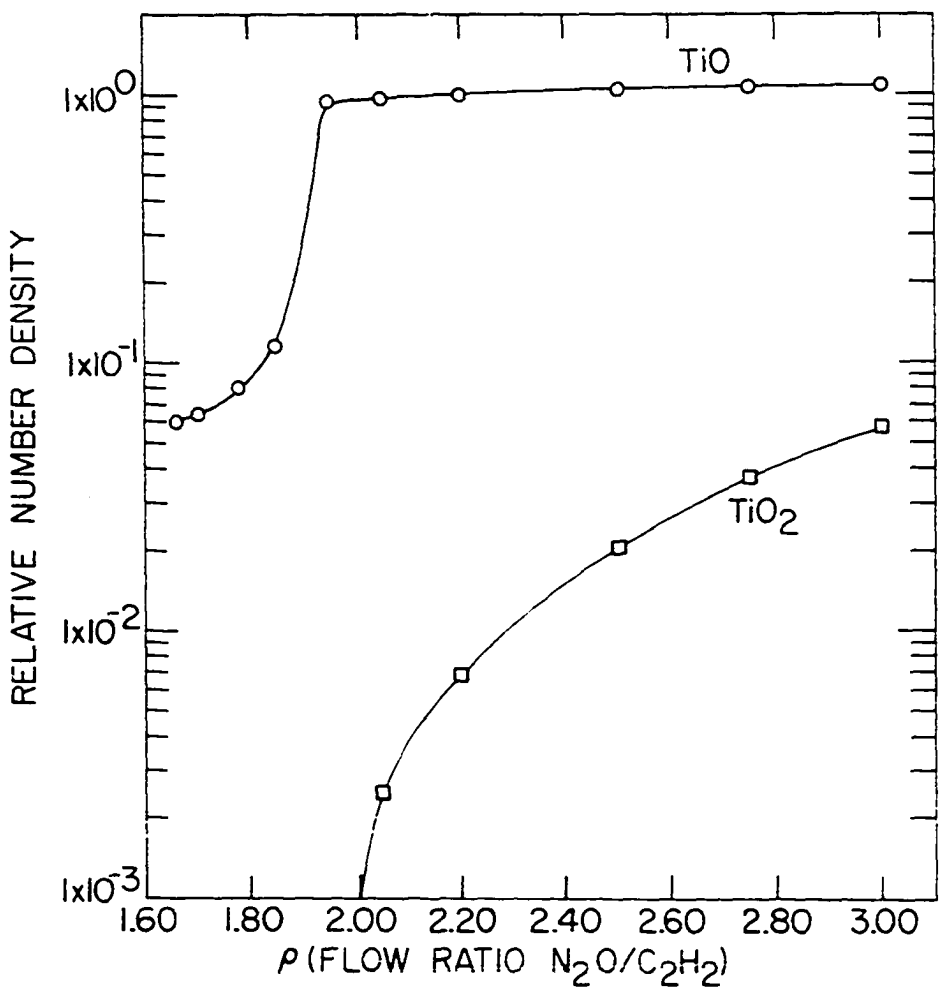

Figure 21. Predicted Ti compound formation at 6 mm above the burner as a function of ρ

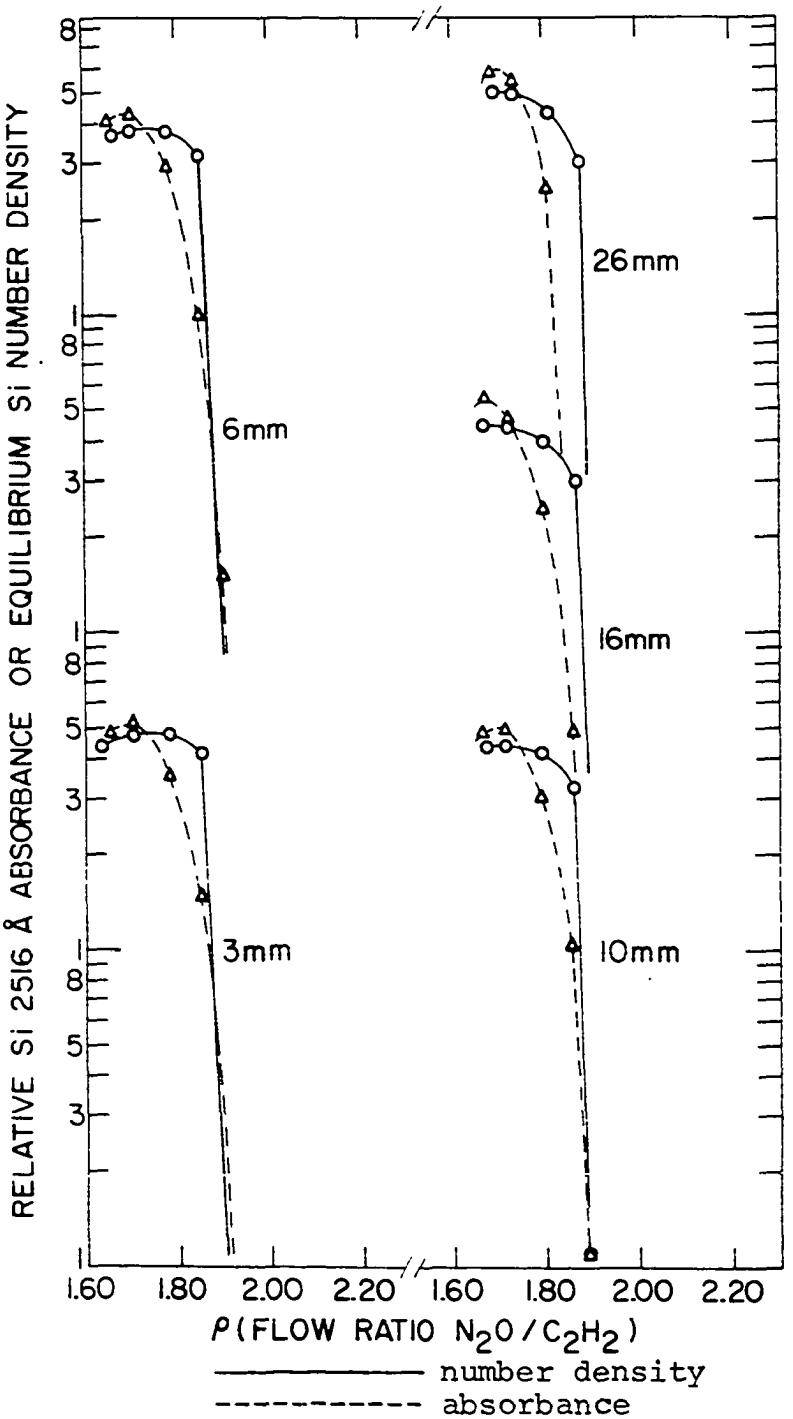

Figure 22. Relative Si absorbances and predicted metal number densities at selected heights above the burner as a function of ρ

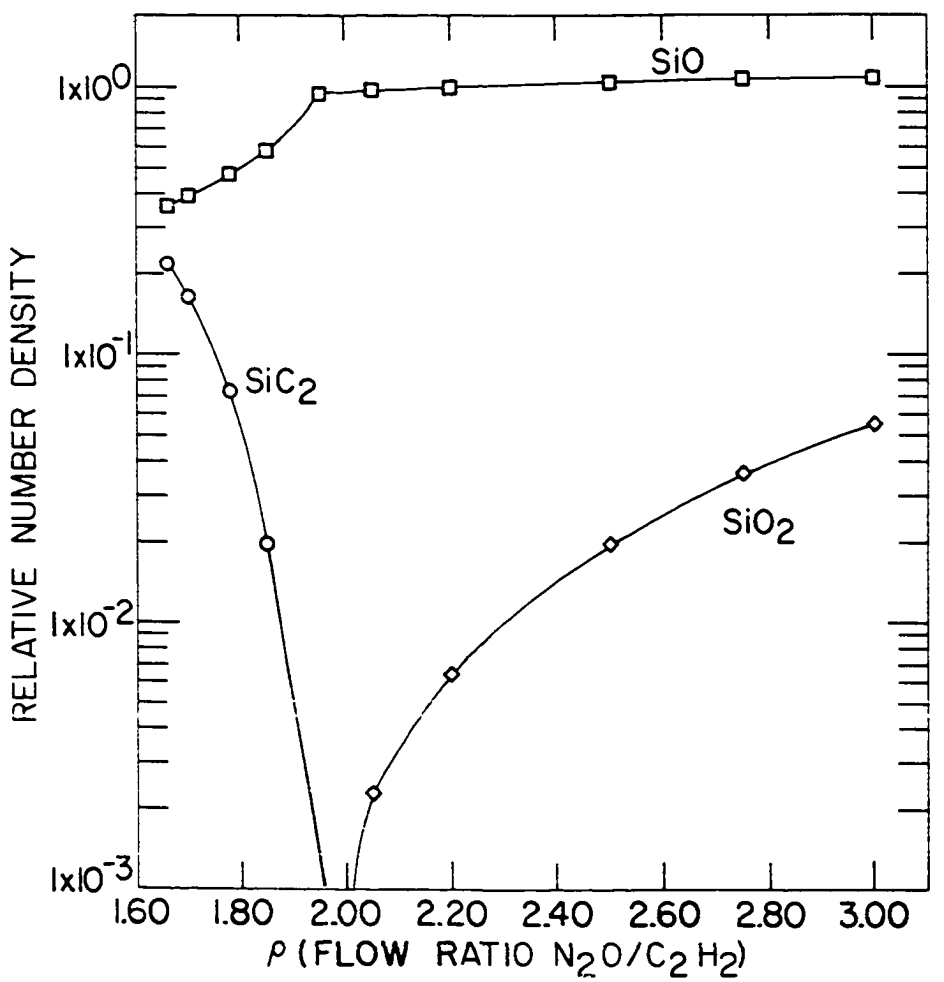

Figure 23. Predicted Si compound formation at 6 mm above the burner as a function of ρ

However, the sample input rate into the flame was assumed to not change with ρ. But, as discussed previously, the dilution effects, which result from changes in: flame temperature, the total N_2O-C_2H_2 flow rate, and the calculated ratio of the total flow rate of N_2O and C_2H_2 to the flow rate of the flame gases after combustion, change the number density of the metal in all its forms as ρ varies. Thus, the resulting metal compound number density curves only approximately represent the degree of compound formation at values of ρ other than 1.66.

The ten metals may be divided into two broad groups. Figures 7 through 13 represent the atomization behavior for elements (Cu, Fe, Mg, Na, and Li) that do not form extremely stable compounds with oxygen; the metals represented in Figures 14 to 23 (Al, Be, W, Ti and Si) show the converse behavior.

1. Types of compounds formed

That the most significant metal compound which influences metal atomization is the monoxide may be confirmed by examination of the figures representing those elements that form very stable oxygen compounds (Figures 14 to 23). Of these elements, Be and W offer some exception. Figure 17 reveals that the hydroxide and dihydroxide of Be should determine the degree of atomization for Be. The approximate agreement between the shapes of the calculated and

experimental curves of Figure 16 supports the accuracy of the predictions of Figure 17. Although W forms a very stable monoxide, Figure 19 reveals that W may react with the flame gases to produce a complex mixture of oxygen-containing species.

The largest surprise of this study was the apparent formation of stable carbon-metal compounds in the carbon-rich flame. Figure 11 illustrates that NaCN may be formed in larger concentrations relative to the concentration of free Na atoms than any other sodium compound. The Na-number-density experimental and predicted curves of Figure 10 reflect the apparent NaCN formation. Figure 12 reveals that Li absorbances decrease in an analogous manner in the carbon-rich flame except that the decreases are even more pronounced. Although no thermodynamic data were available for LiCN, this compound may have been formed in the carbon-rich flame because: (a) next to CO, the most stable carbon species in the N_2O-C_2H_2 flame is HCN (Figure 5); since Li lies between H and Na in the periodic table, LiCN may be more stable than NaCN; (b) the magnitude of the loss of Li free atoms in the carbon-rich flame and the fact that Li salts are completely vaporized in flames that are more than 500° cooler (12) seem to rule out a solute-vaporization explanation of the phenomenon. The experimental data of Figure 12, however, do not preclude the possibility that some other carbon-

containing Li compound was formed in the carbon-rich flame. That other varieties of metal compounds containing carbon may form in this flame is, indeed, suggested by Figure 23, which reveals that Si, SiO, and SiC_2 should have about equal partial pressures in a N_2O-C_2H_2 flame that is slightly more fuel-rich than the most fuel-rich flame employed in this study. Although the shapes of the Si absorbance curves of Figure 22 are not in conflict with the predicted formation of SiC_2, the influence of SiC_2 formation on Si atomization cannot be unambiguously verified. Ca and Si (78) as well as Ba (42) absorbances are also depressed in carbon-rich flames in a somewhat analogous manner to the behavior of Na and Li. Although to our knowledge this possibility has not been reported in the literature, metal-carbon compound formation may not be a rarity. In a similar manner to the reduction of metal monoxides in carbon-rich flames, metal-carbon compounds should be rather completely oxidized to the free metal and other metal compounds in leaner flames.

2. Equilibration of metal-compound-formation processes

As discussed in the introduction, whether free radical disequilibrium can alter the concentration ratio of free metal atoms to metal compounds depends upon the dominant reaction mechanism(s) producing and destroying the metal compound(s). Thus, the question of the degree that natural

flame species in the N_2O-C_2H_2 flame achieve the equilibrium state cannot be unambiguously answered by studying the behavior of metal free atom production because the dominant atomization mechanisms are not known. But, to the flame spectroscopist more important questions are: (a) what degrees of metal atomization are predicted for the flame at equilibrium,and (b) to what extent does metal atomization achieve the equilibrium state in the N_2O-C_2H_2 flame.

The absorbance behavior of Cu, Fe, and Na (Figures 7, 8, and 10) closely follows the predicted relative number density curves for these respective elements. The parallel between the theoretical and experimental curves of these figures confirms that non-realization of assumptions 8 to 11 of Table 3 did not cause appreciable deviant behavior for these elements and, thus, should not have caused disagreements between the calculated and experimental behavior for the other elements. For example, if the fraction of nebulized aerosol that reached the flame depended markedly on the total flow of nitrous oxide and acetylene through the mixing chamber, much more disagreement would be found in Figures 7, 8, and 10.

Of the first group of elements studied, only Li and Mg absorbances significantly deviated from the relative predicted number density curves (Figures 9 and 12). At greater heights in the flame (greater times of flame

reaction), there was little or no improvement of the agreement between theory and experiment. Accordingly, disequilibrium cannot explain these deviations. Thus, the atomization behavior of Cu, Fe, Mg, Na, and Li is probably described by the equilibrium state.

In contrast to the behavior of the first-group metals, the relative absorbance curves of Al, Be, W, Ti, and Si (Figures 14, 16, 18, 20, and 22) reflect a lower degree of metal atomization than the theoretical curves; this can be seen from the following discussion. Because the calculated [O] decreased steadily with decreases in ρ, a relatively constant degree of metal atomization in the carbon-rich flame as a function of ρ would indicate that the metal is almost completely atomized if the only significant metal compounds formed in the flame contained oxygen. Thus, the relatively flat predicted Al, Be, W, and Ti number density curves for the carbon-rich flame indicate that the calculations based on the flame model predicted virtually complete atomization for these elements at all heights above the burner in the carbon-rich flame. The exact results of these calculations are shown in Table 7 for a height of 6 mm above the burner and a ρ value of 1.66. Although the calculations predicted substantially more Al atomization in the hydrogen-rich flame than realized by experiment (Figure 14), the

Table 7. Computed β-factors (uncorrected) at ρ equal to 1.66 and at a flame temperature of 2814 K

Element	β-factor
Cu	1.00
Fe	1.00
Mg	0.99
Na	0.77
Li	0.92
Al	0.97
Be	0.98
W	0.97
Ti	0.94
Si	0.40

relatively constant absorbances at 10 mm, in the range of ρ values between 1.66 and 1.85, indicate that AlO may have been reduced sufficiently to allow virtually complete Al atomization. The slight decrease in Al atomization in the carbon-rich flame at 6 mm as ρ decreased probably reflects either incomplete solute vaporization or some degree of metal-carbon compound formation. For Be, W, Ti and Si (Figures 16, 18, 20, and 22) the absorbance curves increase with decreasing ρ until ρ becomes less than 1.7. Thus, for any of these metals in a flame with a value of ρ between ∿1.7 and ∿1.95, the experimental results indicate that the degree of

atomization was certainly less than that predicted on the basis of the carbon-rich flame model, and for a value of ρ less than $\sim$1.7, the degree of atomization may have been less than the predicted value. (Because of (a) the close agreement between the theoretical and experimental curves for Cu and Fe and (b) the agreement found in the carbon-rich flame for Mg absorbances, the β-factors found in Table 7 for these elements are probably accurate. There is some uncertainty in the value for Na and β for Li is obviously in error at this particular stoichiometry.) An estimation of the actual β-factors for all ten elements will be found in a later section.

For the second group of elements (Al, Be, W, Ti, and Si) deviations between the predicted number-density curves and experimental absorbance curves were most severe high in the flame; this suggests that free radical disequilibrium or a time-decay in the establishment of the equilibrium values of [M]/[MO] was not primarily responsible for these aberrations because: (a) supra-equilibrium concentrations of free radicals are most likely to be found close to the primary reaction zone; and (b) higher heights in the flame allow reactions involving metal atoms more time to reach completion. Conversely, disagreement low in the flame between results of the calculations and experiment but agreement higher in the flame would have suggested the likely

possibility of disequilibrium. Unfortunately, the divergence of the calculated and experimental curves rendered the detection of minor disequilibria to be impossible.

As mentioned in the previous chapter, the assumption that soot is pure graphite and is formed only in equilibrium amounts may not be completely valid. However, the calculations did not predict significant formation of soot at the ρ values employed in this study at heights up to 26 mm above the burner. Moreover, the presence of soot could not be visually observed at any height in the center of the flame even for the richest flame studied.

If soot were formed in the region of the flame where spectroscopic observations were made, the soot formation would most likely occur high in the flame where the temperature is lower. A valid question that should be answered at this point is whether soot formation can explain the worse agreement between predicted metal number densities and relative absorbances for Al, Be, W, Si and Ti at higher heights in the flame.

If soot were formed at any ρ value at a particular height in the flame, a decrease in that ρ should produce more soot and a further contribution to the temperature decrease. At the same time, the atomic oxygen level should remain reasonably constant because in the equilibrium expression

$$[O] = \frac{[CO]}{K_{CO}[C]}$$

where K_{CO} is the equilibrium formation constant for CO from C and O (K_{CO} increases with decreasing temperature but [C] in equilibrium with solid carbon decreases with decreasing temperature). Because, the formation constant, K_{MO}, for the metal monoxide species, MO, increases with decreasing temperature and because

$$\frac{[M]}{[MO]} = \frac{1}{[O]K_{MO}}$$

the degree of atomization for a metal monoxide forming element should either remain constant or decrease when soot is present and ρ decreases. In Figures 14, 16, 18, 20, and 22, the experimental absorbances for Al, Be, W, Ti, and Si all increase at 26 mm above the tip of the burner when ρ decreases in the carbon-rich flame even though soot is most likely to be formed at such a height. Thus, the conclusion is that soot did not form in the region of the flame where spectroscopic observations were made.

If soot were formed prematurely (in a manner not predicted by the equilibrium state), the picture presented in the preceding paragraph would be distorted somewhat. However, if this were the case, when the value of ρ at which soot just started to form was made smaller, the reducing properties of

the flame would probably decrease or remain the same: the likely result of such a decrease in ρ would just be the production of more soot with little or no change in [O]. Because premature carbon formation occurs in premixed N_2O-C_3H_8 flames, for example, no absorption for Al, Si or Ti could be detected in the flame regardless of stoichiometry (60). Consequently, the possibility that soot formation caused the experimental absorbance curves to deviate from the predicted metal number density curves appears extremely remote.

As an incidental point, this evidence for the absence of soot at ρ values greater than 1.65 is in conflict with De Galan's and Samaey's statement (60) that soot is formed in N_2O-C_2H_2 flames at "the critical C/O ratio" of 1.0, which corresponds to a ρ value of 2.0.

Another assumption, which should be examined critically, is that solute vaporization was complete for the elements studied. To assist in this evaluation, metal absorbances as a function of height in the flame are presented in Figure 24. The elements of the first group (Fe, Na, Mg, Cu, and Li) are represented in the left-hand portion of Figure 24. The vertical absorbance profiles for these elements are relatively constant above 6 mm with the exception of Li. The more rapid decrease in Li absorbance as a function of height above the burner was probably caused by a faster rate of diffusion for the light Li atoms away from the center of the flame. If solute vaporization were not

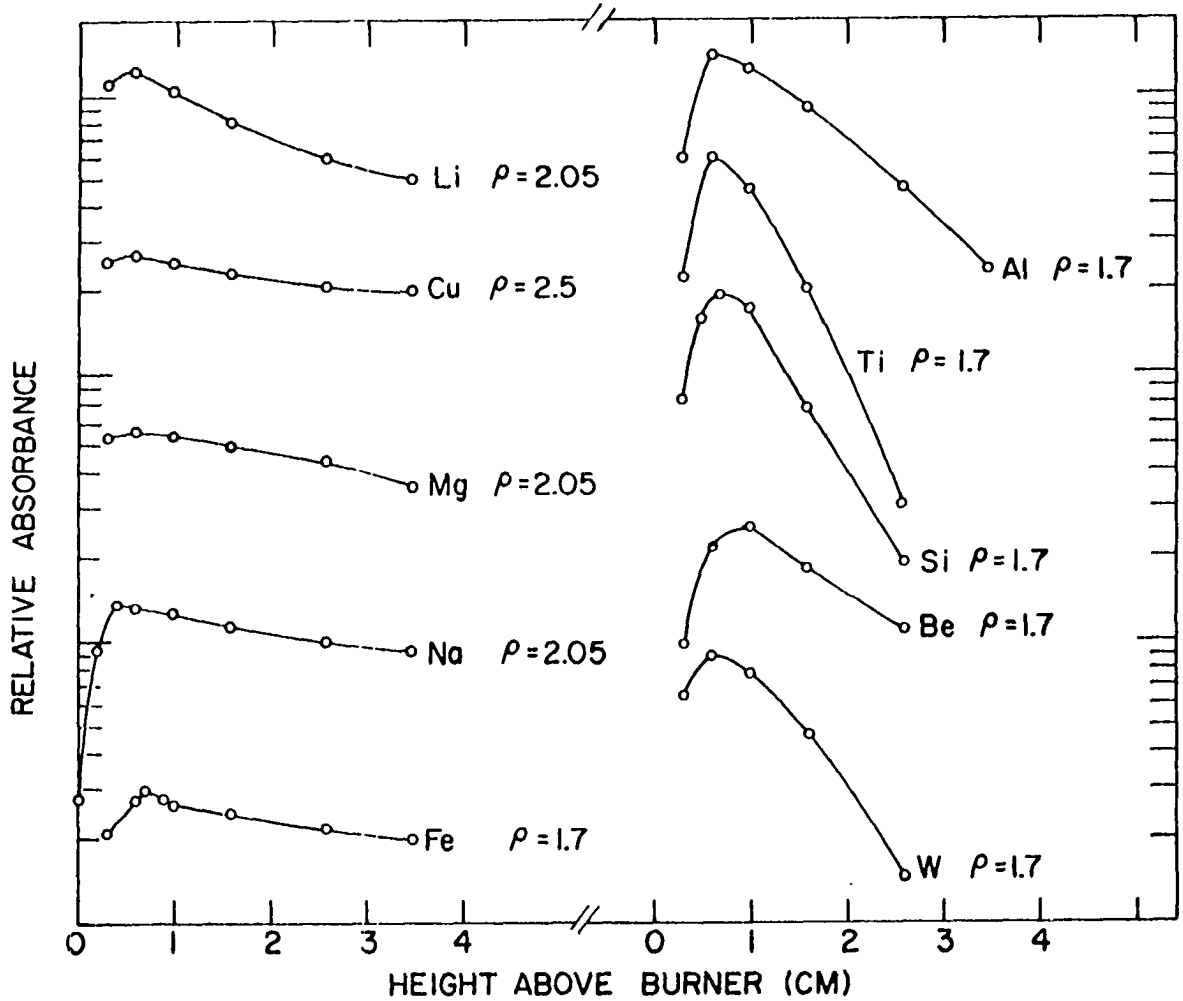

Figure 24. Vertical absorbance profiles

complete at 6 mm and above for Fe, Na, Mg, and Cu, their vertical absorbance profiles would not have the identical shapes shown in Figure 24; this is because the degree of solute vaporization for these elements would have slowly increased at differing rates as height of observation in the flame was increased. Moreover, the degree of metal atomization depends markedly on ρ, the flame temperature, and the height of observation when solute vaporization is incomplete (23). Further evidences of complete solute vaporization for the first group of elements are thus: (a) the relatively flat absorbance curves (Figures 7 to 10 and 12) found for these metals, and (b) the fact that, in general, improvements between theory and experiment were not found at higher heights in the flame; the lessening of the decrease of Li absorbances in the carbon-rich flame (Figure 12) with height in the flame may have been caused by a slower rate of diffusion of the heavier LiCN molecules from the center of the flame as compared to the lighter Li atoms.

Whether solute vaporization was also complete at 6 mm for the second groups of elements (W, Be, Si, Ti, and Al) cannot be easily determined from the vertical profiles of Figure 24. This data for these metals, however, does confirm that the actual degrees of atomization, at least high in the carbon-rich flame, are lower than those predicted since, at a ρ value of 1.7, virtually complete atomization (except

for Si) was predicted for all heights of observation up to 26 mm.

There are, nevertheless, three arguments supporting the contention that solute vaporization was completed reasonably low in the flame for the second group of elements. First, as indicated in the introduction, statements in the literature (36, 47-51) suggest that the N_2O-C_2H_2 flame is relatively free of solute vaporization interferences. For example, Becker (47) has shown that many solute vaporization interferences can be avoided by use of this flame. In addition, the use of the fluoride ion in solution with Ti assured maximal Ti solute vaporization (36). Secondly, except for Al, fair agreement between the theoretical and experimental curves for the second groups of metals was obtained at 6 and 10 mm above the tip of the burner (Figures 16, 18, 20, and 22). The striking lack of agreement between the predicted Ti number density and absorbance curves at 3 mm is probably indicative of substantially incomplete solute vaporization. Moreover, since deviations between the absorbance and predicted number density curves were greater high in the flame than at 6 mm, incomplete solute vaporization apparently was not responsible for the shortcomings of the model. Thirdly, according to Willis (68), straight analytical curves found, at 6 mm, for all elements except Be, implies complete solute vaporization. Because of these arguments and the sharp

maxima for the Al, Ti, Si, and Be vertical profiles of Figure 24, solute vaporization is believed to have been either complete or quite substantial at these maxima (6 mm above the burner for Al, Ti, Si, and W and 10 mm, for Be).

3. Some contradictions in the literature

The literature review of the introduction and, to some extent, the experimental results indicate that the degree of atomization in the premixed N_2O-C_2H_2 flame can be described by the corresponding equilibrium state. Certain interpretations of interelement enhancements found in the literature are in direct conflict with these indications.

For example, Robinson and co-workers (79, 80) found that Ti and Al concomitants enhanced V absorbance, that Ti enhanced Al absorbance, and that V had no effect on Al absorption. Their interpretation (79) for this behavior in the N_2O-C_2H_2 flame was that an atomic oxygen concentration decrease caused by reactions of the kind

$$Ti + O \rightarrow TiO$$

shifted equilibria such as

$$V + O \rightleftarrows VO$$

to the left. Interpreting their data in this manner, Ramakrishna, West, and Robinson (80) concluded that the results suggested that the stabilities of the metal monoxides

"...are most probably in the order Ti > Al > V."

Marks and Welcher (81) have provided some further support for the hypothesis of Robinson et al. They not only found that Ti enhanced Al absorption but that AlO emission was correspondingly decreased. However, little effect of an Al concomitant was found on TiO emission, but an Al on Ti absorption enhancement was reported. Marks and Welcher concluded "... that competition for oxygen may account for some of the enhancement effects... The competition probably occurs in the solid or liquid phase before salt evaporation is complete."

Several questions may be posed on the tenability of the oxygen-competition hypothesis. First, that such small concentrations (10^{-7} atm is a reasonable estimate) of metals in the flame gases would significantly alter the flame environment, especially with regard to analyte atomization processes, seems most unlikely: It is highly improbable that the [M] to [MO] ratio is established via a reaction mechanism directly involving atomic oxygen. Even reaction mechanisms [11] and [12] suggested by Kirkbright et al. (35) appear more probable than a reaction of the type

$$M + O + X \rightleftarrows MO + X$$

primarily because [O] should be lower than 10^{-8} atm in the interconal zone (as shown in the next section). Moreover,

the partial pressure of any metal in the flame is likely to be a few orders of magnitude smaller than the partial pressures of carbon-containing species (Figure 5) that are capable of reacting with a metal monoxide to cause equilibration of the [M] to [MO] ratio. Consequently, the metal could not react with enough of the carbon-containing free radicals to upset the equilibrium ratio of [M] to [MO] even if the reaction were extremely slow. Secondly, even if the somewhat implausible argument of oxygen competition in the liquid phase (81) is valid, the results reported in this manuscript would not support the premise of a serious lag in the establishment, after vaporization of the solute, of the equilibrium [M]/[MO] value. Finally, Marks and Welcher's (81) experimental evidence supporting the oxygen-competition hypothesis is somewhat inconsistent. For example, 200 ppm Al as a concomitant enhanced Ti free-atom absorbances 45%; if, on the other hand, Ti reduced AlO by oxygen-competition, the absorbance of Ti should have decreased with the addition of the Al concomitant. Another inconsistency is that the increase in Ti absorbance by concomitant Al was accompanied by an unchanged TiO emission signal. Willis (82) also has criticized the oxygen-competition hypothesis on the basis of the fact that concomitant Fe, with a low monoxide stability, enhances Ti absorption. Whatever the correct interpretation of these enhancements

may be, it is hoped that this discussion will inspire further work to resolve these questions.

The viewpoint that metal atomization reaches equilibrium in premixed N_2O-C_2H_2 flames is also inconsistent with the deductions of Sastri, Chakrabarti, and Willis (83). Enhancements for Ta, Hf, Nb, and Zr absorbances were found when the formation of analyte metal-oxygen bonds in solution were prevented by the addition of organic complexing reagents. Although organic solvents are known to enhance free atom production, these increases in sensitivity are most often ascribed to: (a) smaller droplet formation that allows a higher percentage of the analyte to pass through the spray chamber and/or (b) greater solute vaporization efficiencies. In certain instances, however, the complexing reagents employed by Sastri et al. to enhance free atom production were too low in concentration to affect the physical properties of the solution.

Sastri et al., in interpreting their observations on the basis of a time delay in the conversion of stable gaseous metal oxides to free metal atoms, stated that "... the MO species [a metal bonded directly to oxygen in a complexing molecule] in the solution contributes greatly to the total amount of metal oxide in the flame, and hence, reduces greatly the population of the free metal atoms in the flame. How-

ever, if the metal atoms can be present in the solution without being bonded to oxygen, as in metallocenes, then the total amount of the metal oxide is formed entirely in the flame, as a result of the equilibrium..." that involves the metal atoms with the flame gases. Sastri et al. admitted that differing solute vaporization rates may explain some of their results. However, they noted that metal acetylacetonates (metal bonded directly to oxygen atoms in the organic ligand) and metallocenes (no oxygen in the organic ligand) should both be easily volatilized but that the metallocene yielded a more intense atomic spectral line than an acetylacetonate complex for the same metal.

The interpretations made by Sastri et al. to explain their data are also somewhat questionable. First, metal compound formation and dissociation would not be expected to proceed at a slow enough rate to easily detect gross disequilibrium effects. Secondly, Zr, Hf, Ta, and Nb, the only metals that were studied by Sastri et al. in the premixed N_2O-C_2H_2 flame, are known to form rather refractory solid oxides (84). An alternative to the Sastri et al. interpretation is that when oxygen is bonded directly to the metal as in acetylacetonates, solid oxides may form as decomposition products of the heated organo-metallic complexes. Further work is also required, however, to satisfactorily explain these free atom enhancements.

E. β-Factors of Metals in the Nitrous Oxide-Acetylene Flame

To critically evaluate the efficiency of the N_2O-C_2H_2 flame as an atomization cell, it is necessary to accurately measure the degree of analyte conversion to free atoms. As discussed in the introduction, attempts to measure this quantity (the β-factor) spectroscopically have achieved limited success. In this section, the results of the calculations based on the flame model will be modified to account for experimental discrepancies, and β-factors for the elements of this study will be calculated as a result of the modifications.

By the process of elimination, incomplete validity of the last two assumptions of Table 3 was believed to be the cause for the discrepancies between theory and experiment. These assumptions were: (a) that all possible flame species are considered in the model and (b) that all thermodynamic data are accurate. This is not meant to imply that some unconsidered source could not have been responsible for these discrepancies. As described in the previous section, it was also concluded that the degrees of atomization for Al, Be, W, Ti, and Si appeared in general to be less than the predicted values. The behavior of these elements in the carbon-rich flame could have been the result of: (a) <u>all</u> the flame model equilibrium formation constants for AlO,

BeOH or $Be(OH)_2$, WO, TiO, and SiO were too low; or (b) the calculated values for [O] in the carbon-rich flame were too low. Of these two possibilities the latter seemed more probable.

An appropriate modification in the calculations thus seemed to be an increase in the values of [O] for the carbon-rich flame. The assumption was made that the calculated values of [O] for the carbon-rich flame were too low by the same factor at all values of ρ. Some support for this assumption was found by altering a natural-flame-molecule formation constant by a definite factor at all values of ρ for the carbon-rich flame. This was done individually for most of the major and a few of the minor species of the carbon-rich flame so that [O] was increased by a factor of $\sim$5 or more in each case. The temperatures at 6 mm were assumed for these calculations. The ratio of the altered values for [O] to the originally calculated values for [O] remained constant to within 30% as ρ varied between 1.66 and 1.85 regardless of the formation constant that was altered. (A ρ value of 1.95 corresponded to the transition between carbon-rich and hydrogen-rich flames since the nebulized H_2O added oxygen to the flame.)

Thus, theoretical number density curves as a function of ρ for Na, W, Ti, and Si were computer drawn for values of [O] that were increased by factors of 2, 4, 8, 16, 32, 64 and 128.

[O] was increased by these factors **only** for the carbon-rich flame (ρ=1.66 to 1.95) at 6 mm above the burner. Number density curves for Al and Be were not drawn in this manner because the Al experimental absorbance and theoretical number density curves as a function of ρ deviated more than for any other element, and a straight analytical curve was not found for Be. The multiplications of [O] by the factor, O.F., was accompanied by a division of [C] by O.F. This division assumed that the equilibrium formation constant for CO was correct and was a result of the equilibrium

$$C + O \rightleftarrows CO.$$

The original unaltered values for [O] and [C] that were predicted for the height of 6 mm above the burner as a function of ρ are presented in Figure 25. The partial pressures of N_2 and H_2 were not changed during these manipulations. Out of the eight number density curves representing O.F. values from 1 to 128, one was selected that best matched the experimental absorbance curve measured at 6 mm. This was done for each of the four elements.

Figure 26 illustrates the improved agreement (over Figures 18, 20, and 22) between the altered theoretical number density curves and the absorbance curves for W, Ti, and Si. Because of the possibility of small errors in the measurement of ρ, the experimental curves were shifted

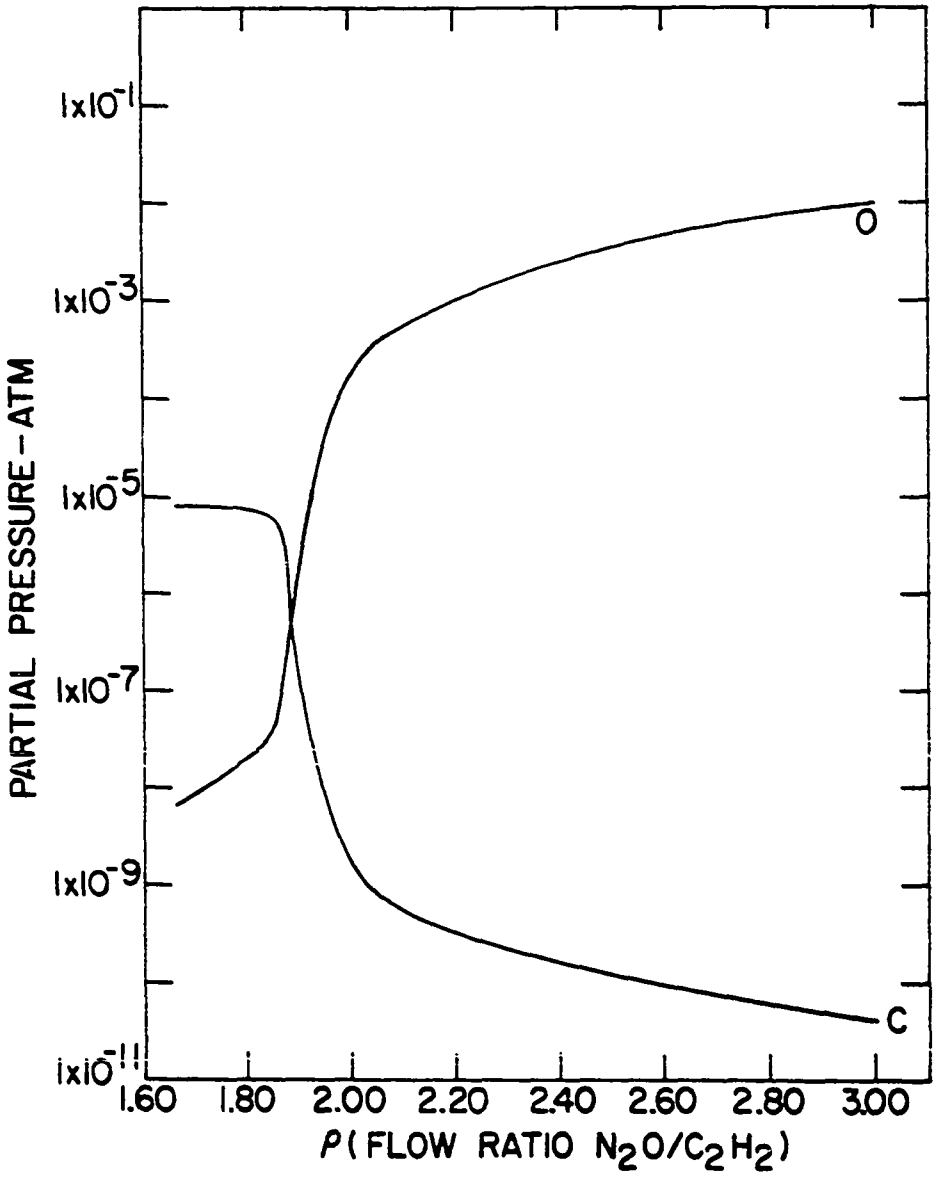

Figure 25. Predicted values for [C] and [O] at 6 mm above the burner tip as a function of ρ

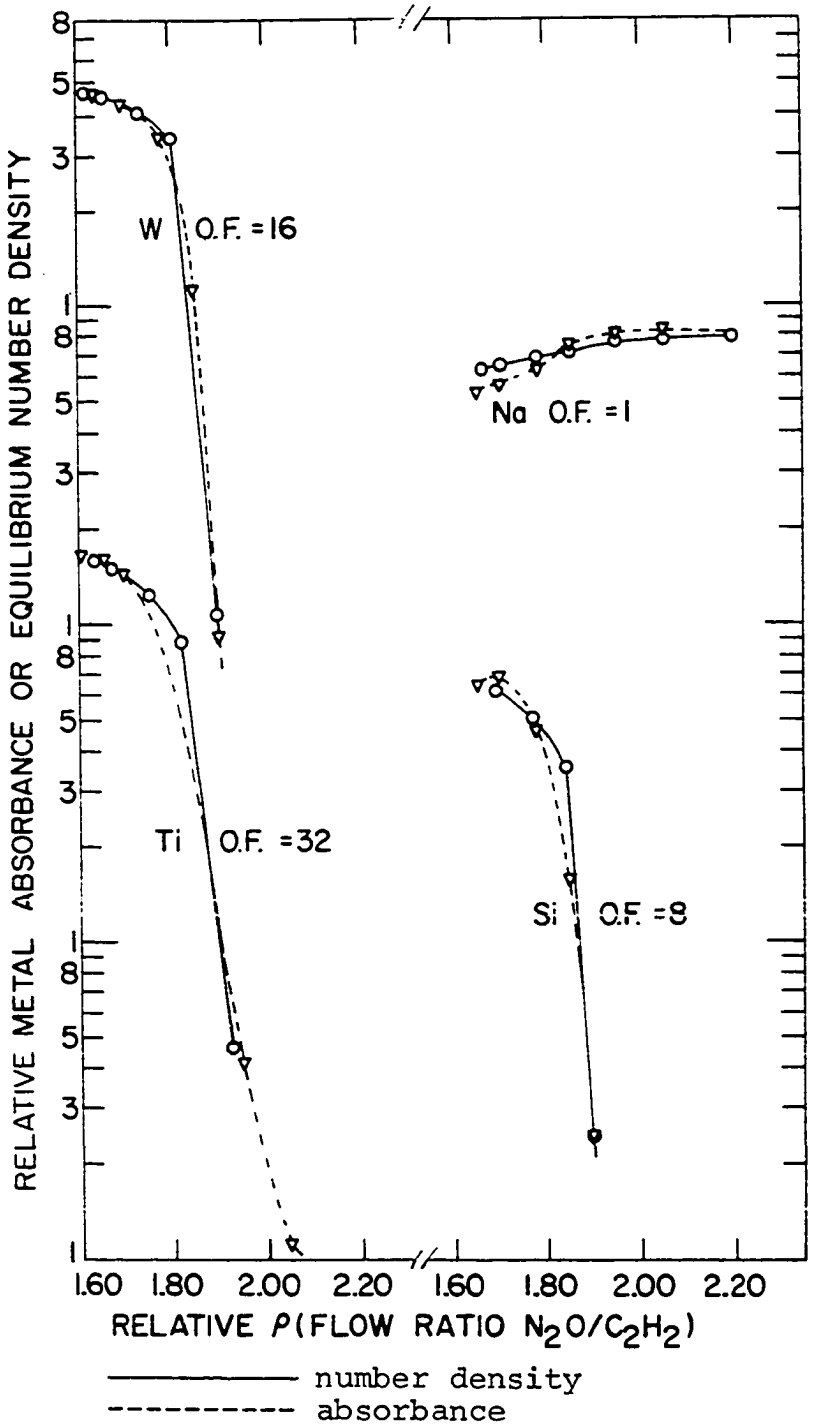

Figure 26. Absorbance and modified number density curves at 6 mm as a function of ρ. O.F. refers to a linear factor that atomic oxygen was increased

slightly (less than 0.05 ρ units) in the horizontal direction to optimize the curve fit. For this reason, the values of ρ in Figure 26 were labeled "relative". The accuracy to which O.F. could be determined for each of the elements was to within a factor of 2. The atomization behavior for Na in the carbon-rich flame seems to be an exception to the behavior for the other three elements because the best curve-fit was found for the unaltered calculations. The variation of the O.F. factors for the W, Ti, and Si curves may reflect small errors in the monoxide formation constants for these elements. As an example of the large uncertainties associated with the thermodynamic data reported for some metal compounds, the range of the dissociation energies for AlO is from 4.6 to 5.9 eV (62). (It is an interesting sidelight to note that the upper limit of the AlO dissociation energies was determined by a flame method. The results of this manuscript would also support a value that was in the high part of this range. However, the Al absorbance curves plotted as a function of ρ may have been influenced by an oxygen-containing Al compound that was not included in the flame model.) An O.F. value of 16, however, yielded reasonable agreement for each of the W, Ti, and Si curves of Figure 26. For this reason, it was concluded that values for [O] in the carbon-rich flame may be a factor of ∿16 too low. Consequently, the original predicted values for

[O] were multiplied by a factor of 16 for the calculation of β-factors for the carbon-rich flame. The original values for [O] that were calculated for the hydrogen-rich flame were assumed to be accurate.

Table 8 lists the resulting calculated β-factors for values of ρ that yielded maximal atomization. For Si and Ti, two β-factors are shown, which reflect both the O.F. value of 16 and the O.F. values for the respective elements in Figure 26. The shapes of the experimental absorbance-versus-ρ curves were also considered when the optimal values for ρ were selected. For example, the calculations based on the flame model did not predict loss of Li atomization in the carbon-rich flame but the experimental results (Figure 12) precluded ρ values less than 1.95 for Li. The reason that not all of the β-factors for Al through Na were exactly 1 was because of various calculated degrees of metal hydride formation.

An obvious question at this point is how accurate are the calculated β-factors of Table 8 in view of the obvious uncertainty in the experimental O.F. value of 16. Figure 27 illustrates calculated β-factors for Be and Ti as a function of O.F. at 6 mm above the burner and with a ρ value equal to 1.66. A similar curve for W would lie between the Be and Ti curves, and a curve for Si would be somewhat below the Ti curve. Similar curves for all the other metals studied

Table 8. Nitrous oxide-acetylene β-factors for a height of 6 mm above the burner tip as a function of the monoxide dissociation energy

Metal	β	ρ	$D_{0_{MO}}$ (eV) (61)
Si	0.065-0.12	1.66	8.24
Ti	0.33-0.49	1.66	7.27
W	0.71	1.66	6.95
Al	0.97	1.66	4.99
Be[a]	0.98	1.66	4.60
Fe	1.00	1.66-1.95	4.25
Mg	0.99	1.66-1.95	4.03
Cu	1.00	1.66-2.05	3.56
Li	0.96	1.95	3.34
Na	0.99	1.95	3.09

[a]Solute vaporization was apparently not complete for Be at 6 mm.

would be located along the Be curve (if metal-carbon compound formation is ignored). Thus, an uncertainty in O.F. of a factor of 2 causes a relatively large uncertainty in the calculated β-factor for Si and smaller uncertainties in the β-factors for Ti and W. Most of the elements studied would still have calculated β-factors near 1 in the carbon-rich flame even if the calculated [O] were increased by several

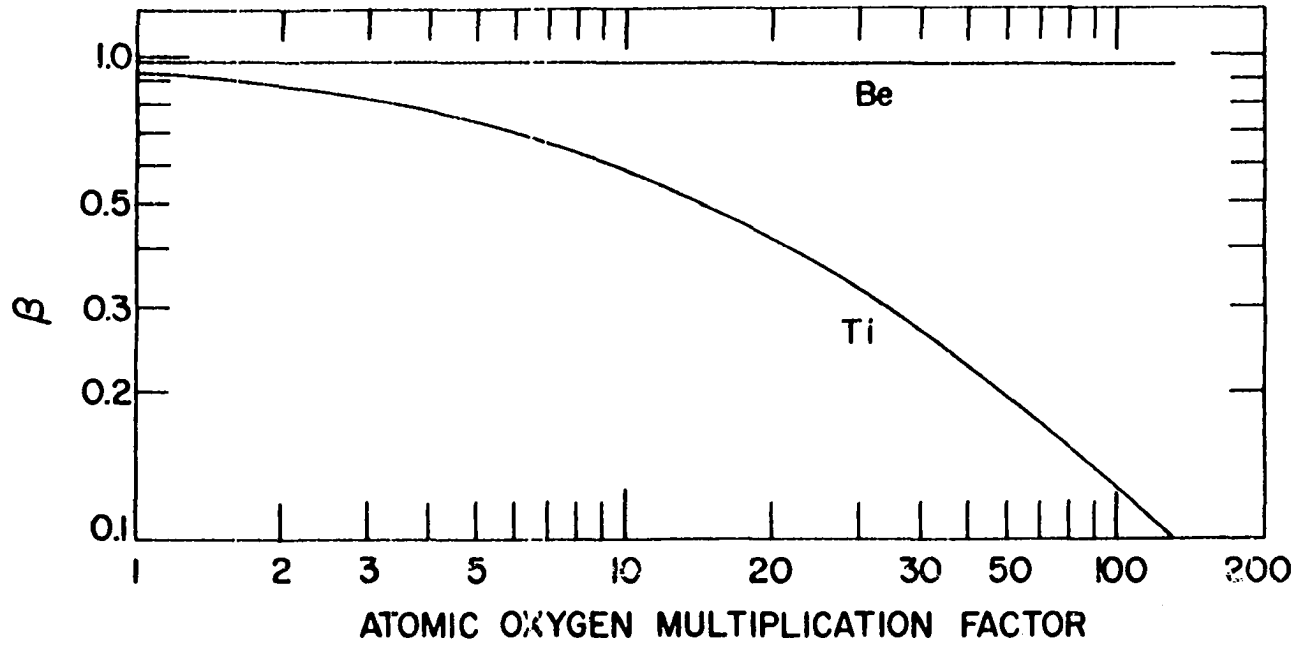

Figure 27. Calculated β-factors for Be and Ti as a function of multiplying the predicted values of [O] at 6 mm and at ρ equal to 1.66

orders of magnitude. The β-factors shown in Table 8, therefore, strongly imply that, in general, when solute vaporization is complete, a value ρ exists at which atomization is complete for metals that form monoxides with dissociation energies less than ∿6.5 eV.

To satisfactorily account for the loss in atomization for Ti, Si, and W at higher heights in the flame, O.F. values that are from 5 to 15 times greater than those of Figure 26 are necessary (for the height of 26 mm above the burner). No explanation seemed completely satisfactory to explain this behavior. Consequently, this problem is left for future workers to solve.

F. Practical Applications

An ideal flame for the quantitative determination of trace metals should: (a) possess the ability to completely atomize all elements, (b) have a high enough flame temperature to completely vaporize the sample, (c) contribute little spectral background radiation or absorption, and (d) be safe, convenient, and inexpensive to operate.

Both premixed N_2O-H_2 (85) and O_2-H_2 flames (86) compare favorably with regard to categories (b) through (d). These flames possess little emission or absorption background except from the OH molecule. A very fuel-rich O_2-H_2 flame

does not emit much OH radiation but the flame temperature may be as low as 2000 K (86). Regardless of flame stoichiometry, these hydrogen flames are not capable of efficiently atomizing elements that form stable monoxides (60, 85, 86). In fact, the maximum calculated β-factor for Ti in the premixed O_2-H_2 flame is $\sim 5 \times 10^{-5}$ (86).

The premixed N_2O-C_2H_2 flame, on the other hand, rates highly in categories (a), (b), and (d) on a comparison basis. However, the flame possesses extensive emission and absorption from CH, NH, NO, and C_2 but especially CN and OH (35, 65). High intensity of background radiation not only increases photomultiplier "noise" but at times "buries" an atomic emission line in structure. For atomic absorption, the loss in signal from a hollow cathode lamp because of background absorption decreases the signal to noise ratio (65). Thus, the ability to control background emission and absorption is an obvious requirement to optimize analyses in this flame. The use of a good-resolution monochromator for emission measurements is one way to improve the signal to background ratio and aids in the identification of spectral lines.

More direct regulation of N_2O-C_2H_2 flame background can be effected by critically monitoring ρ. The dependence of the partial pressures of the spectroscopically observed species upon ρ is illustrated in Figure 6. Although the

chemical environment of the edges of an unshielded flame from a slot burner does not reflect the ρ value because of secondary combustion with air, careful adjustment of the cross-section of the flame viewed by the monochromator should minimize the effect of the entrained air. Thus, the contributions of the flame edges should only manifest itself at the ends of the flame, and the long observational path length through the flame should encounter a chemically uniform environment. The geometrical configuration of slot flames, therefore, is more conducive to critically monitoring ρ to adjust the flame background than the geometry of cylindrical flames. If the flame reaches approximate concentration equilibrium, Figure 6 reflects the stoichiometries required to suppress radiation or absorption from any of the species except NH. A flame with minimal background and a relatively high temperature should be attainable at a value of ρ corresponding to the intersection of the CN and OH curves plotted in Figure 6. Of course, the minimization of flame background ought to be tempered with considerations for the ability of the flame to produce free atoms of the analyte. In practice, because of (a) the highly localized nature of distributions of free atoms for many elements in unshielded flames (42) and (b) the sensitivity of relative free-atom populations of these elements to changes in ρ, the selection of optimum values for ρ and heights of

observation in the flame should be the best compromise to allow the lowest possible detection limits.

The conclusion that when solute vaporization is complete, there exists a value of ρ at which atomization is complete for metals that form monoxides with dissociation energies less than $\sim$6.5 eV is rigidly valid only when a small cross-section area of the flame is viewed by the monochromator. Moreover, the exact value of ρ at which complete atomization should occur may differ from the values shown in Table 8 because of the effects of air entrainment. However, in practice, it may be possible to atomize Si, Ti, and W more extensively than Table 8 indicates because unshielded flames do not "lift-off" the burner at ρ values less than 1.66.

IV. LITERATURE CITED

1. Snelleman, W., A flame as a standard of temperature, Unpublished Ph.D. thesis, Utrecht, Holland, University of Utrecht, 1965.

2. Hollander, Tj., Amer. Inst. Aeronaut. Astronaut. J., 6, 385 (1968).

3. Alkemade, C. Th. J., in "Tenth Colloquium Spectroscopicum Internationale", Spartan Books, Washington, D.C., 1963, p. 143.

4. Hollander, Tj., Self-absorption, ionization and dissociation of metal vapor in flames, Unpublished Ph.D. thesis, Utrecht, Holland, University of Utrecht, 1964.

5. Hooymayers, H. P. and C. Th. J. Alkemade, J. Quant. Spectrosc. Radiat. Transfer, 6, 501 (1966).

6. Gaydon, A. G. and H. G. Wolfhard, "Flames, their structure, radiation, and temperature", 2nd edition, Chapman and Hall Ltd., London, England, 1960.

7. Shuler, K. E., in "Seventh Symposium (International) on Combustion", Butterworth Scientific Publications, London, England, 1959, p. 87.

8. Jenkins, D. R. and T. M. Sugden, in "Flame Emission and Atomic Absorption Spectrometry, Volume 1--Theory", Dean, J. A. and T. C. Rains, eds., Marcel Dekker, Inc., New York, N.Y., 1969, Chapter 5.

9. Alkemade, C. Th. J., A contribution to the development of flame photometry, Unpublished Ph.D. thesis, Utrecht, Holland, University of Utrecht, 1954.

10. Fenimore, C. P. and G. W. Jones, J. Phys. Chem., 62, 693 (1958).

11. Fenimore, C. P. and G. W. Jones, J. Phys. Chem., 62, 1578 (1958).

12. Bulewicz, E. M., C. G. James and T. M. Sugden, Proc. Roy. Soc., A235, 89 (1956).

13. Kaskan, W. E., Combust. Flame, 2, 229 (1958).

14. Kaskan, W. E., Combust. Flame, 2, 286 (1958).

15. Schott, G. L., J. Chem. Phys., 32, 710 (1960).

16. Zeegers, P. J. Th. and C. Th. J. Alkemade, Combust. Flame, 5, 247 (1965).

17. Zeegers, P. J. Th., Recombination of radicals and related effects in flames, Unpublished Ph.D. thesis, Utrecht, Holland, University of Utrecht, 1966.

18. McEwan, M. J. and L. F. Phillips, Combust. Flame, 11, 63 (1967).

19. Sugden, T. M., in "Annual Review of Physical Chemistry", Eyring, H., C. J. Christensen and H. S. Johnston, Eds., Annual Reviews Inc., Palo Alto, California, 1962, Vol. 13, p. 369.

20. Schofield, K. and T. M. Sugden, in "Tenth Symposium (International) on Combustion, The Combustion Institute, Pittsburgh, Penn., 1965, p. 589.

21. Fenimore, C. P. and G. W. Jones, J. Phys. Chem., 62, 178 (1958).

22. Pungor, E. and I. Cornides, in "Emission and Atomic Absorption Spectrometry, Volume 1--Theory", Dean, J. A. and T. C. Rains, Eds., Marcel Dekker, Inc., New York, N.Y., 1969, Chapter 3.

23. Alkemade, C. Th. J., in "Flame Emission and Atomic Absorption Spectrometry, Volume 1--Theory", Dean, J. A. and T. C. Rains, Eds., Marcel Dekker, Inc., New York, N.Y., 1969, Chapter 4.

24. Gaydon, A. G. and H. G. Wolfhard, Proc. Roy. Soc., A205, 118 (1951).

25. Willis, J. B., J. O. Rasmuson, R. N. Kniseley, and V. A. Fassel, Spectrochim. Acta, 23B, 725 (1968).

26. Reif, I., To appear in Ph.D. thesis, Ames, Iowa, Library, Iowa State University, ca. 1971.

27. Gilbert, P. T., in "Tenth Colloquium Spectroscopicum International," Lippincott, E. R. and M. Margoshes, Eds., Spartan Books, Washington, D.C., 1963, p. 171.

28. Broida, H. P. and Schuler, K. E., J. Chem. Phys., 27, 933 (1957).

29. Gibson, G. H., W. E. L. Grossman, and W. D. Cooke, Anal. Chem., 35, 266 (1963).

30. Dean, J. A. and Simms, J. C., Anal. Chem., 35, 699 (1963).

31. Bulewicz, E. M., Combust. Flame, 11, 297, (1967).

32. Bulewicz, E. M. and P. J. Padley, Combust. Flame, 5, 331 (1961).

33. Bulewicz, E. M. and P. J. Padley, in "Ninth Symposium (International) on Combustion," Academic Press, New York, N.Y., 1963, p. 638.

34. Miller, W. J., Oxidation and Combustion Revs., 3, 97 (1968).

35. Kirkbright, G. F., M. K. Peters, and T. S. West, Talanta, 14, 789 (1968).

36. Amos, M. D. and J. B. Willis, Spectrochim. Acta, 22, 1325 (1966).

37. Amos, M. D. and P. E. Thomas, Anal. Chim. Acta, 32, 139 (1965).

38. Fassel, V. A., R. H. Curry, and R. N. Kniseley, Spectrochim. Acta, 18, 1127 (1962).

39. Cowley, T. G., V. A. Fassel, and R. N. Kniseley, Spectrochim. Acta, 23B, 771 (1968).

40. L'vov, B. V., "Atomic Absorption Spectroscopy" (Translated from Russian), Israel Program for Scientific Translations, Jerusalem, 1969.

41. Anderson, C. H., Pittsburgh Conference on Analytical Chemistry and Applied Spectroscopy, Cleveland, Ohio, March 1968.

42. Fassel, V. A., J. O. Rasmuson, R. N. Kniseley, and T. G. Cowley, Relative Free-Atom Populations in Nitrous Oxide-Acetylene Flames Used in Analytical Spectroscopy, Spectrochim. Acta, in press.

43. Bulewicz, E. M. and T. M. Sugden, Trans. Far. Soc., 55, 770 (1959).

44. Sugden, T. M., Trans. Far. Soc., 52, 1465 (1956).

45. Bulewicz, E. M. and T. M. Sugden, Trans. Far. Soc., 52, 1481 (1956).

46. Fiorino, J. A., R. N. Kniseley, and V. A. Fassel, Spectrochim. Acta, 23B, 413 (1968).

47. Becker, D. A., Chemical interferences and ionization in high temperature flames, Unpublished Ph.D. thesis, Ames, Iowa, Library, Iowa State University, 1970.

48. Fassel, V. A. and D. A. Becker, Anal. Chem., 41, 1522 (1962).

49. Pickett, E. E. and S. R. Koirtyohann, Spectrochim. Acta, 23B, 235 (1968).

50. Koirtyohann, S. R. and E. E. Pickett, Spectrochim. Acta, 23B, 673 (1968).

51. Pickett, E. E. and S. R. Koirtyohann, Spectrochim. Acta, 24B, 325 (1969).

52. De Galan, L. and J. D. Winefordner, J. Quant. Spectrosc. Radiat. Transfer, 7, 251 (1967).

53. Koirtyohann, S. R. and E. E. Pickett, in "Thirteenth Colloquium Spectroscopicium International", Adam Hilger Ltd., London, England, 1968, p. 270.

54. Willis, J. B., Atomization Problems in Atomic Spectroscopy. II. Determination of Degree of Atomization in Premixed Flames, Spectrochim. Acta, in press.

55. Zeeger, P. J. Th., W. P. Townsend, and J. D. Winefordner, Spectrochim. Acta, 24B, 243 (1969).

56. Hinnov, E. and H. Kohn, J. Opt. Soc. Am., 47, 156 (1957).

57. Hofmann, F. W. and H. Kohn, J. Opt. Soc. Am., 51, 512 (1961).

58. Willis, J. B., Atomization Problems in Atomic Absorption Spectroscopy. III. Absolute atomization efficiencies of sodium, copper, silver, and gold in a Meker-type air-acetylene flame, Submitted for publication in Spectrochim. Acta, ca. 1970.

59. Rann, C. S., Spectrochim. Acta, 23B, 827 (1968).

60. De Galan, L. and G. F. Samaey, Spectrochim. Acta, 25B, 245 (1970).

61. JANAF Thermochemical Tables, prepared by Dow Chemical Company, Midland, Michigan. Clearinghouse for Federal Scientific and Technical Information, PB-168370, 1966-69.

62. Gaydon, A. G., "Dissociation Energies and Spectra of Diatomic Molecules", 3rd ed., Chapman and Hall, London, England, 1968.

63. Walsh, A., Spectrochim. Acta, 7, 108 (1955).

64. Veillon, C. and J. Y. Park, Anal. Chem., 42, 684 (1970).

65. Fiorino, J. A., Molecular absorption and light scattering in flames employed for atomic absorption spectroscopy, Unpublished Ph.D. thesis, Ames, Iowa, Library, Iowa State University, 1970.

66. Sasaki, Y., J. Appl. Phys., 5, 439 (1966).

67. Kadyshevich, A. E., Usp. Fiz. Nauk, 76, 683 (1962).

68. Willis, J. B., Spectrochim. Acta, 23A, 811 (1967).

69. De Waele, M. and W. Harjadi, Anal. Chim. Acta, 23B, 725 (1968).

70. Kniseley, R. N., in "Flame Emission and Atomic Absorption Spectrometry, Volume 1--Theory," Dean, J. A. and T. C. Rains, Eds., Marcel Dekker, Inc., New York, N.Y., 1969, Chapter 6.

71. Strehlow, R. A., "Fundamentals of Combustion", International Textbook Co., Scranton, Penn., 1968.

72. Pitzer, K. S. and E. C. Clementi, J.A.C.S., 81, 4477 (1959).

73. Fenimore, C. P., in "The International Encyclopedia of Physical Chemistry and Chemical Physics," Guggenheim, E. A., J. E. Mayer, and F. C. Tompkins, Eds., The Macmillan Company, New York, N.Y., 1964, Vol. 5.

74. Homann, K. H., Combust. Flame, 11, 265 (1967).

75. Snelleman, W., in "Flame Emission and Atomic Absorption Spectrometry, Volume 1--Theory," Dean, J. A. and T. C. Rains, Eds., Marcel Dekker, Inc., New York, N.Y., 1969, Chapter 7.

76. Willis, J. B., Iowa State University, personal communication, 1968.

77. Bulewicz, E. M. and P. J. Padley, Trans. Far. Soc., 65, 186 (1969).

78. Becker, D. A., Iowa State University, personal communication, Ames, Iowa, 1969.

79. Sachdev, S. L., J. W. Robinson, and P. W. West, Anal. Chim. Acta, 37, 12 (1967).

80. Ramakrishna, T. V., P. W. West, and J. W. Robinson, Anal. Chim. Acta, 39, 81 (1967).

81. Marks, J. Y. and G. G. Welcher, Anal. Chem., 42, 1033 (1970).

82. Willis, J. B., Applied Optics, 7, 1295 (1968).

83. Sastri, V. S., C. L. Chakrabarti, and D. E. Willis, Can J. Chem., 47, 587 (1969).

84. Handbook of Chemistry and Physics, 50th edition, Weast, R. C., Ed., Chemical Rubber Publishing Co., Cleveland, Ohio, 1969.

85. Willis, J. B., V. A. Fassel, and J. A. Fiorino, Spectrochim. Acta, 24B, 157 (1969).

86. Mossholder, N. V., Spectroscopic properties and analytical applications of premixed oxygen-hydrogen flames, Unpublished Ph.D. thesis, Ames, Iowa, Library, Iowa State University, 1970.

V. ACKNOWLEDGMENTS

To Dr. Velmer A. Fassel, under whose guidance I have worked for the past four years, I would like to express appreciation for patience and encouragement. The many hours that Dr. Fassel spent reading this manuscript and his many helpful suggestions are also gratefully acknowledged.

Thanks are also extended to both past and present members of our research group for their friendship and many valuable discussions. Special thanks must be given to Mr. Richard N. Kniseley who was always willing to generously donate his time to help solve any problem.

My gratitude to both my wife's parents and my own for their help cannot be adequately expressed.

Finally, I would like to thank my wife, Sue, and my children, Jeannine and Eric, for their loving patience. They fulfill my life to a degree that scientific pursuits cannot approach.